The Release and Dispersion of Gas from Pipeline Ruptures

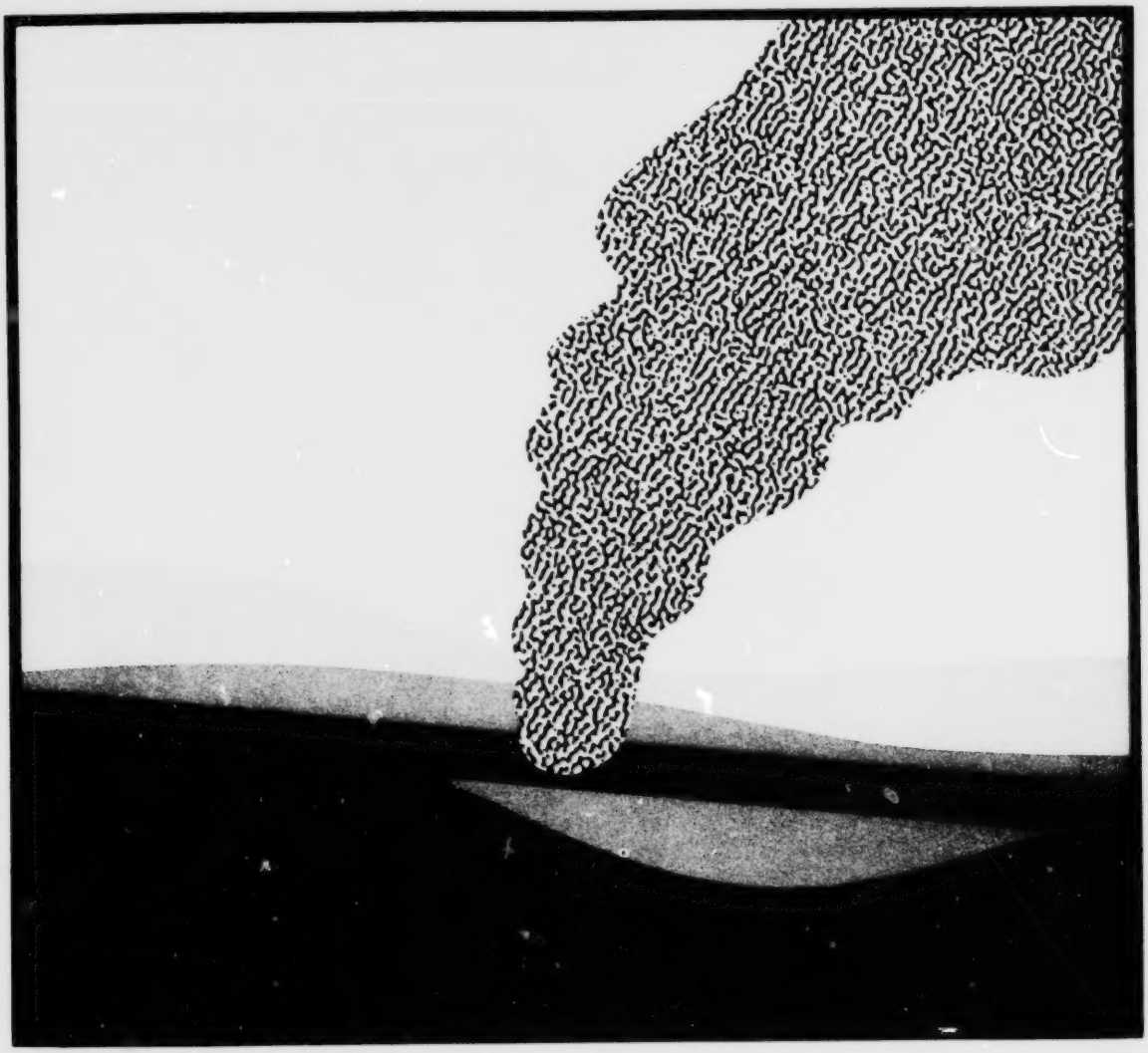

Alberta

ENVIRONMENT

87-01014/

THE RELEASE AND DISPERSION OF GAS FROM PIPELINE RUPTURES

By

D.J. Wilson
Department of Mechanical Engineering
University of Alberta
Edmonton, Alberta, Canada

prepared for

ALBERTA ENVIRONMENT
9820 - 106 Street
Edmonton, Alberta T5K 2J6

Project Officer: R.P. Angle
Air Quality Control Branch
Pollution Control Division
Environmental Protection Services

Contract No. 790686

January 1979

(reissued April 1986)

Table of Contents

SECTION I	STUDY OBJECTIVES	1
	- Sensitivity to Input Parameter Variations	2
	- "Best Estimates" and "Recommended Values"	3
	- New Developments	3
SECTION II	PREDICTING TRANSIENT RELEASE RATES FROM RUPTURES	4
	- Adiabatic Flow Analysis of Initial Moving-Wave Transient	5
	- Isothermal Flow Analysis of Initial Moving-Wave Transient	8
	- Isothermal Release During Fixed Length Blowdown	13
	- Recommended Model for Release Rate	16
SECTION III	SONIC JET EXPANSION OUTSIDE THE RUPTURE	17
	- Including the Effect of Turbulence Kinetic Energy	19
	- Choosing the Source Exit Area A_s	21
	- Incompressible Approximation for Source Velocity	21
	- Numerical Example	24
SECTION IV	GAUSSIAN PLUME MODEL WITH DOWNWIND DIFFUSION OF SOURCE TRANSIENTS	26
	- The Effect of Along-Wind Diffusion on a Plume	27
	- Approximations for x Direction Diffusion	28

- Effective Plume Model 31
- Effective Source Strength $\bar{m}$ for Exponential Release Rate 32
- Numerical Example 33

SECTION V STANDARD METEROLOGICAL CONDITIONS FOR DISPERSION ANALYSIS OF PIPELINE RUPTURES 37
- Surface Roughness and Wind Speed Power Law 38
- Selecting Mean Wind Speed U 40
- Potential Temperature Gradients 40
- Effective Wind Speed for Diffusion 42

SECTION VI PLUME RISE FROM A GROUND LEVEL SOURCE 44
- Final Buoyancy and Momentum Rise 45
- Final Rise in Stable Conditions 47
- Downwind Location of Final Rise 49
- Flow Rate for Plume Rise Analysis 49
- Sensitivity of Ground Level Concentration to Plume Rise 51

SECTION VII SPREADING RATES OF PLUMES 54
- Vertical Plume Spread σ_z 54
- Crosswind Plume Spread σ_y 56
- Along-Wind Plume Spread σ_x 59
- Plume Spread from Self-Generated Turbulence 63

SECTION VIII INDOOR-OUTDOOR CONCENTRATION RATIOS 67

- Analytical Modelling for Indoor-Outdoor Ratios 69
- Exponential Decay of Outdoor Concentration 71
- Building Infiltration Rates 72
- Maximum Indoor Concentration 74
- Effect of Outdoor Concentration Fluctuations 75
- Numerical Example 75

SECTION IX CONCENTRATION FLUCTUATIONS AND PROBABILITY DISTRIBUTIONS 78

- Log-normal Probability Distribution 78
- Fluctuation Intensity Along the Plume Centre Line 82
- Crosswind Variations in Fluctuation Intensity 83
- Numerical Example 85

REFERENCES 89

SECTION 1
STUDY OBJECTIVES

In order to assess the risk from the rupture of a sour gas pipeline, the diffusion of the gas must be evaluated to determine the concentration-time history of any selected receptor location downwind from the pipeline rupture. The purpose of this study was to determine the proper methods for evaluating the trajectory and dilution of a transient gas release emitted at ground level.

Automatic block valves are used to isolate the segment of pipeline where a rupture occurs. After the block valves have closed the release rate of the sour gas containing hydrogen sulphide (H_2S) rapidly decreases with time. In typical situations with block valves spaced a few miles apart, most of the gas is released in a time interval of a few minutes. In formulating a model for the dispersion process this rapid time transient had to be taken into account.

In addition, the release of a plume at ground level requires the increased turbulence and high wind shear near the ground to be accounted for in determining plume rise and spreading rates. Also, for a ground level release, concentrations close to the source are particularly sensitive to plume rise induced by jet momentum and buoyancy, and to "self-dilution" caused by entrainment of ambient air into the plume due to its own self-generated turbulence. Because the large body of existing literature on plume rise and dispersion is concerned almost exclusively with plumes which are released at a steady rate from stacks high above ground level, it is necessary to alter existing theories and develop new ones to account for the special conditions inherent in a pipe rupture.

Finally, because the dispersion model must be used in risk analysis assessment, the fluctuating nature of ground level concentration has to be

considered. Because for an individual pipe burst the concentration passing a receptor can fluctuate greatly about some statistical average value, the probability of observing a particular concentration has to be assessed in order to allow an accurate estimate of toxic gas effects to be made.

Sensitivity to Input Parameter Variations

Because ground level concentration in atmospheric dispersion is very sensitive to changes in wind speed, plume rise, and plume spreading rates, any estimation procedure which predicts full-scale concentrations at a selected location within a factor of two of observed values, is considered to have done an excellent job. It is more typical for such estimation methods to miss by factors of 10 or more.

In this report there has been a conscious effort to show the sensitivity of observed ground level concentrations to variations in the various input parameters in the diffusion model. Because of the complicated interaction between transient release rate, spreading rates, plume rise and concentration fluctuations, the overall sensitivity could not be determined for any except a few simple cases. However, it will be shown that the sensitivity of the Gaussian dispersion model to input parameters decreases rapidly with distance from the source. In general, the process of estimating concentrations at distances closer than 1 kilometer to the source are subject to a great deal of uncertainty due to the sensitivity of atmospheric dispersion in this zone to small variations in meteorological and source conditions.

"Best Estimates" and "Recommended Values"

This report takes the point of view that it is better to make an estimate, which may at best be an educated guess, than to ignore the effect of a parameter entirely. In particular, the estimates in this report for plume rise and concentration fluctuations contain a number of subjective judgements on the probable form of the relationships which govern these parameters.

An attempt has been made to indicate in the report the variables which are estimated with some degree of subjectivity. In making these subjective judgements an attempt has been made to strike a delicate balance between being sufficiently conservative to account for the uncertainties, without being totally unrealistic.

Looking on the brighter side, many of the variables such as the transient release rate, the influence of downwind dispersion, and indoor-outdoor concentration relationships could be determined with a considerable degree of accuracy.

New Developments

In addition to the modifications made to existing dispersion theories for their application to pipeline ruptures, several new analytical techniques were developed and are discussed. These new developments are:

1. A plume mode which includes downwind dispersion and transient release rate.
2. A method for predicting the relationship between indoor and outdoor concentration.
3. Dilution caused by self-induced turbulent entrainment.
4. A model for rate of release, and for mixing of the jet outside the rupture.
5. Estimates of cross-wind variation in fluctuating concentration.

SECTION 2
PREDICTING TRANSIENT RELEASE RATES FROM RUPTURES

Before any prediction can be made of the atmospheric dispersion from the gas release, the rate of release must be specified. When a long pipeline is ruptured at a single point a very high flow rate will initially result. This high release rate will rapidly decrease as flow begins to move down the pipeline, and fluid friction causes the exit pressure to drop below the initial value before rupture. While the mass flow will drop off continuously with time, we can identify two distinctly different periods in the transient blowdown of a pipeline:

1. Immediately after rupture occurs an expansion wave travels down the pipeline at the speed of sound. The gas in front of this expansion wave is at rest, and does not know that the rupture has yet occurred. The mass flow during this moving wave transient can be approximated as the depletion rate from a reservoir of gas at the initial temperature and pressure of the pipeline, flowing down a length of pipe which increases with time at the rate of the sound of speed. This moving wave transient will be completed when the expansion wave reaches the end of the pipeline after a time t_i

$$t_i = \frac{L}{C_1} \tag{2-1}$$

where
$$C_1 = \sqrt{k\,RT_1} \tag{2-2}$$

C_1 = sonic velocity in pipeline gas, m/s

T_1 = temperature of pipeline gas before rupture ^{o}K

k = ratio of specific heats

R = gas constant N-m/kg^{o}K

L = total length of pipe from rupture to block valve

It is interesting to note that because the speed of sound C_1 depends only on the absolute temperature of the gas, the length of this initial transient will be independent of the pipeline pressure. During this initial transient the flow will adjust itself in order to produce a choked condition at the pipe exit with sonic velocity occurring there.

2. After the expansion wave reaches the end of the pipe the system will behave as a reservoir of fixed size depleting through a hole in one end. Because of frictional resistance the pipeline pressure and gas density will decrease gradually from the closed end, reaching a minimum value at the point of rupture where a sonic velocity will persist until the pipe pressure at the exit has dropped to a value less than about twice the atmospheric pressure.

In this section two flow rate models will be suggested to describe the initial moving wave transient, and the final fixed length depletion. Both of the flow models described represent exact solutions, within the limits of the simplifying assumptions made, and therefore require no empirically determined constants. The major assumption in both flow models is that the system at any instant of time is quasi-steady. The assumption of quasi-steady flow implies that fluid acceleration forces are small compared with those generated by pressure. This assumption is generally valid in gas flows, even for very rapid transients, because the low density of a gas prevents fluid acceleration from causing significant forces.

Adiabatic Flow Analysis of Initial Moving-Wave Transient

The leading edge of the expansion wave travels down the duct at the local speed of sound, typically about 300 meters per second. The flow behind the expansion wave starts at a slow velocity and accelerates down

the duct until it reaches the exit at sonic speed. It will be assumed this process takes place adiabatically. Under these conditions the stagantion temperature (the temperature plus the kinetic energy) remains constant. The steady flow solution for frictional flow in a pipe is given by Shapiro (1953) p 167-168 in the form of parametric equations in terms of Mach number at the upstream end of the pipe. In the case of a pipe rupture, the effective length of the pipe at any time t is given by

$$L_t = C_1 t \tag{2-3}$$

and the Mach number is related to the friction factor by

$$\frac{fL_t}{D} = \frac{1-M^2}{kM^2} + \frac{k+1}{2k} \ln \left[\frac{(k+1)M^2}{2\left(1 + \frac{k-1}{2} M^2\right)} \right] \tag{2-4}$$

f = friction factor of pipe

D = pipe diameter, m

$L_t = C_1 t$, the length of pipe traversed by the moving wave, travelling at the sonic velocity C_1 for time t after rupture

M = Mach number behind expansion wave

The stagnation pressure needed to compute the mass release is

$$\frac{P_1}{P_{oe}} = \frac{1}{M} \left[\frac{2\left(1 + \frac{k-1}{2} M^2\right)}{k+1} \right]^{\frac{k+1}{2(k-1)}} \tag{2-5}$$

P_1 = gas pressure in pipeline before rupture

P_{oe} = stagnation pressure at the pipe exit

The relationships in equations 2-4 and 2-5 make use of the fact that the flow continually adusts itself to produce a Mach number of unity (choked flow)

at the pipe exit. Using these two relations the stagnation pressure at any instant can be computed, and the mass release rate calculated from the choked flow relationship

$$\dot{m}_e = \frac{P_{oe} A_e \sqrt{k}}{\sqrt{RT_1}} \left[\frac{2}{k+1}\right]^{\frac{k+1}{2(k-1)}} \qquad (2\text{-}6)$$

$\dot{m}_e$ = mass release rate from the rupture, kg/sec

A_e = cross sectional area of the pipe, m^2

Because of the parametric nature of the equations 2-4 and 2-5, the mass release rate must be estimated by first assuming a Mach number M, and then computing the time of release which corresponds with this assumed value. This is done by inserting the Mach number M in equation 2-4, and using the resulting length L_t in equation 2-3 to determine the time after release corresponding to this assumed value. This same Mach number is used in equation 2-5 to determine the stagnation pressure P_{oe} and this is then used in 2-6 to determine the mass release rate. For typical pipeline ruptures an initial Mach number of 0.2 should be selected and gradually decreased to a value of about 0.02 at which point the expansion wave will have travelled about 15 kilometers down the line.

Although it is not obvious, equation 2-4 shows that once the moving wave has passed, the Mach number at a given distance from the rupture will always remain the same. Using typical values of friction factor f and specific heat ratio k, equation 2-4 can be used to show that the Mach number decreases from unity at the rupture exit to a value of 0.35 in about 200 pipe diameters. Thus, most of the flow acceleration from rest to sonic velocity occurs in a very short length close to the rupture.

Because the equations used to determine the release rate with adiabatic flow are all in parametric form (in terms of M), it is not possible to derive a single functional relationship for the mass flow rate. This lack of a single equation for $\dot{m}_e$ makes a numerical integration necessary to find to total mass released over a specified time interval. The main use of the adiabatic flow predictions are for comparision with simpler approximations, such as the isothermal analysis that will now be developed.

Isothermal Flow Analysis of Initial Moving-Wave Transient

The adiabatic moving wave transient showed that high speed effects, where the Mach number exceeds 0.35 are confined to a region about 200 diameters in length in front of the point of rupture. For the rest of the pipe, typically 20,000 or more diameters in length, the Mach number will be less than 0.35 and no significant temperature changes will occur due to conversion of internal thermal energy to kinetic energy. If we exclude the short region at the end of the pipe where adiabatic acceleration to the sonic exit velocity occurs, virtually the entire pipeline will remain at constant temperature along its length.

The gas filled pipeline is a closed system whose pressure is decreasing with time. If the gas in the pipe were thermally insulated from its surroundings, its temperature would also decrease as the average presssure in the pipeline dropped. However, the recent series of experiments at Pincher Creek, Alberta in which buried pipelines were ruptured, indicate that the metal pipe and the surrounding overburden act as a thermal reservoir. The pipe walls transfer heat to the moving gas in order to maintain a constant temperature flow during the depletion process. For this reason, the following analysis will assume that the flow remains

isothermal both along the pipe, and during its blowdown time. This assumption, which appears reasonable in light of the experiments, greatly simplifies the problem of determining the flow rate from the rupture.

The sketch below shows the relevant variables for the analysis.

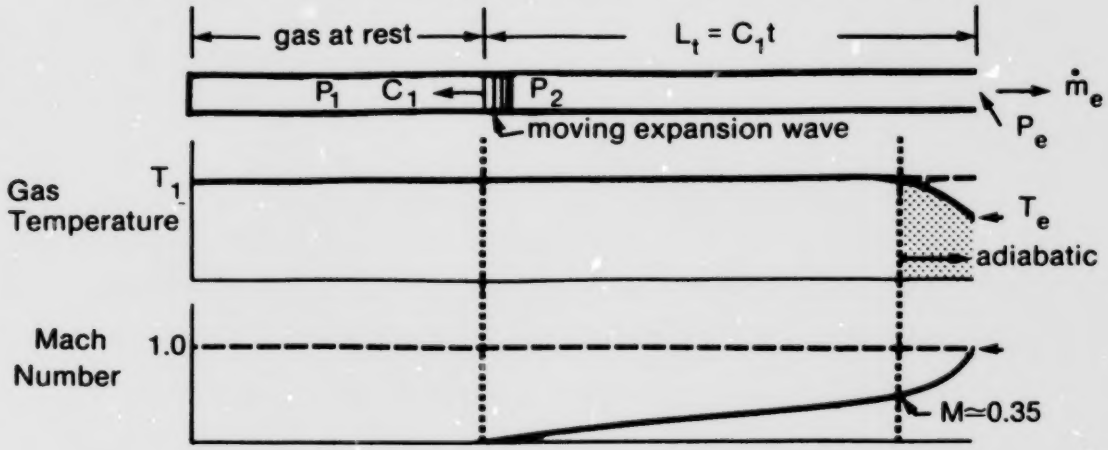

The local pressure gradient at any point in the flow is, in terms of the local velocity V, neglecting accelleration dV/dx caused by density changes,

$$\frac{dP}{dx} = \frac{f}{D} \rho \frac{V^2}{2}$$

For quasi steady flow the mass flow past any point is the same as the exit mass flow. This allows us to write the average velocity as

$$V = \frac{\dot{m}_e}{\rho A_e}$$

From which the pressure gradient is, using the ideal gas law to write $\rho = P/RT$,

$$\frac{dP}{dx} = \frac{f \dot{m}_e^2 RT_1}{2 D P A_e^2}$$

or

$$PdP = \frac{f \dot{m}_e^2 RT_1}{2 D A_e^2} dx$$

Integrating this from the point of rupture $x = 0$, $P = P_e$ to the point behind the moving wave $x = L_t$, $P = P_2$ yields

$$P_2^2 - P_e^2 = \frac{f \dot{m}_e^2 RT_1 L_t}{D A_e^2}$$

At this point an approximation is made which allows the adiabatic choked flow at the rupture exit to be "attached" to the downstream end of the isothermal flow. This approximation is simply that

$$P_2^2 - P_e^2 \cong P_1^2 - P_{oe}^2$$

which will be valid at the moment of rupture and, after the wave has travelled for about 100 diameters ($t \approx 0.1$ sec). After this, the frictional pressure differences along the pipe are much larger than any kinetic energy differences that contribute to the stagnation pressure P_{oe}. The exit stagnation pressure after the expansion wave has travelled for time t, using 2-3 to evaluate L_t.

$$P_{oe} = \left[P_1^2 - \frac{C_1 f \dot{m}_e^2 RT_1 t}{D A_e^2} \right]^{1/2} \qquad (2\text{-}7)$$

To determine the mass release rate the adiabatic choked mass flow at the exit, given by equation 2-6, may be solved for P_{oe} and equated to 2-7. When the resulting equation is solved, the mass release rate is found to be

$$\dot{m}_e = \frac{P_1 A_e}{\sqrt{R T_1}} \left[\frac{1}{k} \left(\frac{k+1}{2} \right)^{\frac{k+1}{k-1}} + \left(\frac{f C_1}{D} \right) t \right]^{-1/2} \qquad (2\text{-}8)$$

This shows that the mass release rate is proportional to $t^{-1/2}$ and reduces to the adiabatic choked flow result at t = 0.

In all the systems considered here the friction factor has been considered as a constant, independent of both time and position along the pipe. In fact, the friction factor for a given pipe is a function of Reynolds number Re_D which is

$$Re_D = \frac{\rho V D}{\mu}$$

$$= \frac{\dot{m}_e}{\pi \mu D}$$

Because $\dot{m}_e$ is constant along the pipe for quasi-steady flow, the assumption that f is constant with x is justified. However, f may vary somewhat as the mass flow decreases with time, causing a proportionate drop in Reynolds number. In turbulent flow, f is only very weakly dependant on Reynolds number and setting it as a constant with time is also reasonable.

The total mass released during the initial transient is W_i from t = o to $t = t_i$ when the moving wave reaches the end of the pipe. The initial mass of gas W_o in the pipe of length L is,

$$W_o = \frac{P_1 A_e L}{R T_1} \qquad (2\text{-}9)$$

Integrating (2-8) the mass released in time t_i is

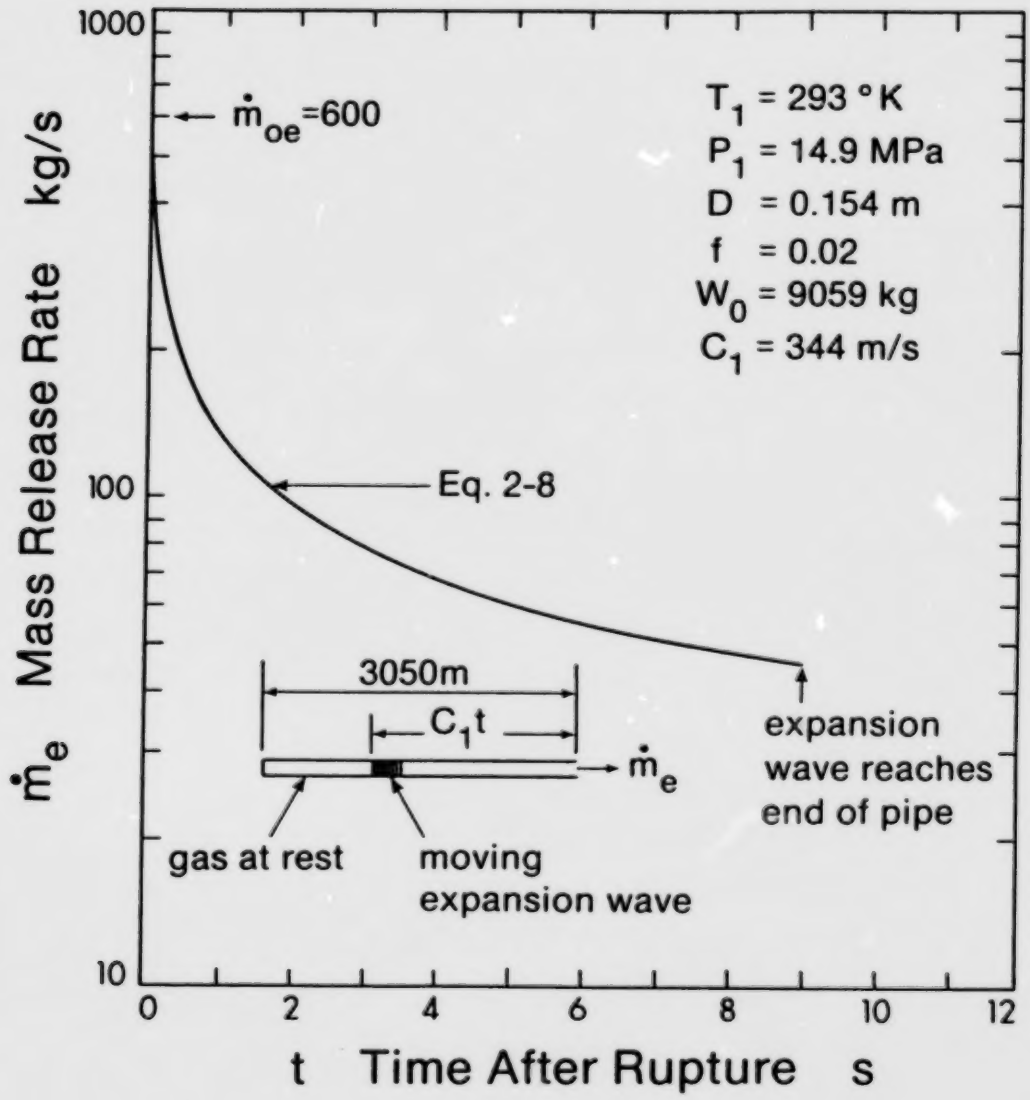

Figure 2-1 Release Rate from Initially Isothermal Pipe. Pipeline Gas with Molecular Weight of $\tilde{M}$ = 25.75 and k = 1.25

$$W_i = \frac{2\,W_o}{\sqrt{k}} \left(\frac{D}{fL}\right) \left[\left(\frac{1}{k} \left(\frac{k+1}{2} \right)^{\frac{k+1}{k-1}} + \frac{fL}{D} \right)^{1/2} - \left(\frac{1}{k} \left(\frac{k+1}{2} \right)^{\frac{k+1}{k-1}} \right)^{1/2} \right] \quad (2\text{-}10)$$

A numerical example has been computed using the preceeding equations and is shown in Figure 2-1. The adiabatic flow model given by equations 2-3 to 2-6 was also used and was found to agree with the isothermal flow rate within a few percent.

Isothermal Release During Fixed Length Blowdown

After the moving wave reaches the end of the pipe, the system behaves as a reservoir of constant volume which is depleting through a hole at one end. The main resistance to this depletion is frictional resistance on the flow moving down the pipe toward the rupture.

An exact solution has becn carried out for the isothermal blowdown of a pipe of length L. Because the density varies with distance along the pipe as the pressure drops from the closed end to the exit, the solution requires a considerable amount of mathematical manipulation to obtain the deceptively simple result that

$$\dot{m}_e = \left[\frac{W_o - W_i}{\beta} \right] \exp\left(\frac{-t}{\beta} \right) \quad (2\text{-}11)$$

The factor β is given by

$$\beta = \delta \left[\frac{kfL}{D} \right]^{1/2} \cdot t_i \quad (2\text{-}12)$$

β = time constant of release rate, sec

W_o = initial mass of gas in pipe before rupture eq. (2-7) kg

W_i = mass of gas released during initial transient, kg

δ = a constant depending on the type of flow = $\frac{2}{3}$ for isothermal flow.

t_i = time for the initial expansion wave to travel down the pipe see eq. 2-1, sec.

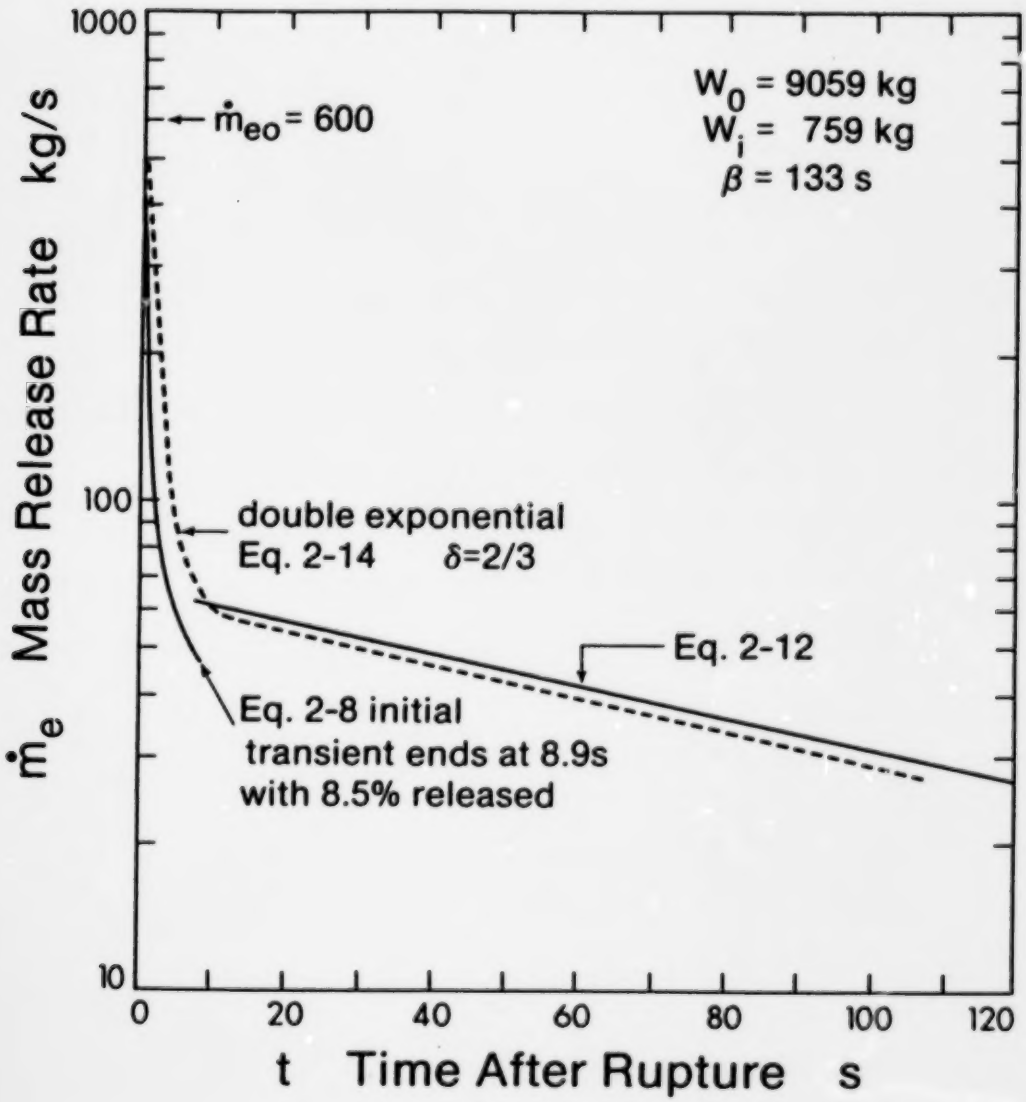

Figure 2-2 Final Fixed Length Isothermal Depletion and Comparison to Double Exponential Approximation (see Fig. 2-1 for release conditions)

Bell (1978) presents a semi-empirical model for release rate, in which he approximates the entire process including the initial transient as a double exponential with two different time constants. His arguments for determining the final time constant are based on a broad physical analogy with stead incompressible flow, he obtains exactly the same form as equations 2-11, 2-12 but with an empirical form for the constant δ in equation 2-12. His choice of this constant is made by fitting the double exponential model to a finite difference computer release rate model (which presumably is thought to be more accurate). He finds the constant to be

$$\delta = 2\left[1 - \exp\left(-26{,}400\,\frac{D}{L}\right)\right]^{1/2} \qquad (2\text{-}13)$$

For typical pipelines which are about 20,000 diameters long equation 2-13 predicts a value of about $\delta \tilde{=} 1.7$ which is much greater than $\delta = 0.67$ indicated by the isothermal flow theory. In spite of this large discrepancy, it is still encouraging that both the semi-emperical and exact isothermal theory predict idential functional forms for the final transient decay rate.

The numerical example shown in Figure 2-1 has been extended in Figure 2-2 to the region of the final fixed length transient. Note that the mass release rate at the end of the initial transient is discontinuous in order that the total mass released will be the initial mass in the pipeline W_o. This discontinuity in release rates can be removed simply by equating the release rates at the time t_i and then multiplying <u>both</u> release rate equations by a factor which adjusts the overall total mass release to W_o.

Recommended Model for Release Rate

While the release rate models developed above for the initial moving wave transient, and the final fixed length depletion, have the advantage that they have no dependence on empirically determined constants, they are not nearly as easy to use as Bell's (1978) double exponential model.

The release rate during the initial moving wave transient is definitely not an exponential, which would appear as a straight line on Figure 2-1. However, this transient persists for such a short time that considering all the uncertainties present during the initial start-up when the overburden is blown off the ruptured pipe, an exponential approximation is probably reasonable. Bell has developed the coefficients of his double exponential form to assure that the total mass released by the double exponential decay rate is equal to the initial mass W_o that was originally in the pipe. Bell derives the double exponential form as

$$\dot{m}_e = \frac{\dot{m}_{oe}}{(1+\alpha)} \left[\exp\left(\frac{-t}{\alpha^2 \beta}\right) + \alpha \exp\left(\frac{-t}{\beta}\right) \right] \qquad (2\text{-}14)$$

$\alpha \equiv \frac{W_o}{\beta \dot{m}_{oe}}$, a mass conservation factor

$\dot{m}_{oe}$ = initial release rate computed from (2-6) with $P_{oe} = P_1$, the initial pipe pressure

W_o = total mass in the pipeline, from (2-9)

β = final release time constant form (2-12) using $\delta = 2/3$, or Bell's δ from (2-13)

Note that with the condition of mass conservation imposed, the time constant of the first exponential is set automatically by the final time constant β.

SECTION 3
SONIC JET EXPANSION OUTSIDE THE RUPTURE

As long as there is sufficient pressure in the pipeline, the flow conditions will adjust themselves to produce choked flow, with sonic velocity at the pipe rupture. Sonic velocity at the pipe exit will be maintained as long as the exit stagnation pressure is more than twice the ambient atmospheric pressure. Because most pipelines operate at pressures of 500 psia or more, this choking condition assures that 90% or more of the mass flow will emerge when the exit flow is at sonic velocity. Only a very small fraction of the total mass in the pipeline will escape during the final transient when the exit stagnation pressure drops too low to maintain sonic speed at the pipe exit.

When the pipe rupture is operating with a sonic exit velocity the pressure at the exit will be higher than the ambient pressure, and the jet will undergo a sudden expansion as it leaves the pipe exit. This expansion and recompression process is followed by subsonic turbulent mixing as shown schematically in Figure 3-1. The processes involved are highly irreversible, and result in a rapid increase in jet temperature as the kinetic energy in the sonic flow at the pipe exit is converted to thermal energy in the flowing gas. Because the mixing process is very rapid, no heat is gained or lost by the jet, and the process is adiabatic with a constant stagnation temperature T_o. In the following analysis it will be shown that if the source area A_s (after the expansion and mixing process has been completed) is specified, the conditions in the exit jet may be computed exactly from adiabatic compressible flow relationships. Finally, a simple approximation to incompressible flow will be made which allows direct computation of the source momentum and buoyancy fluxes without requiring the use of compressible flow relationships.

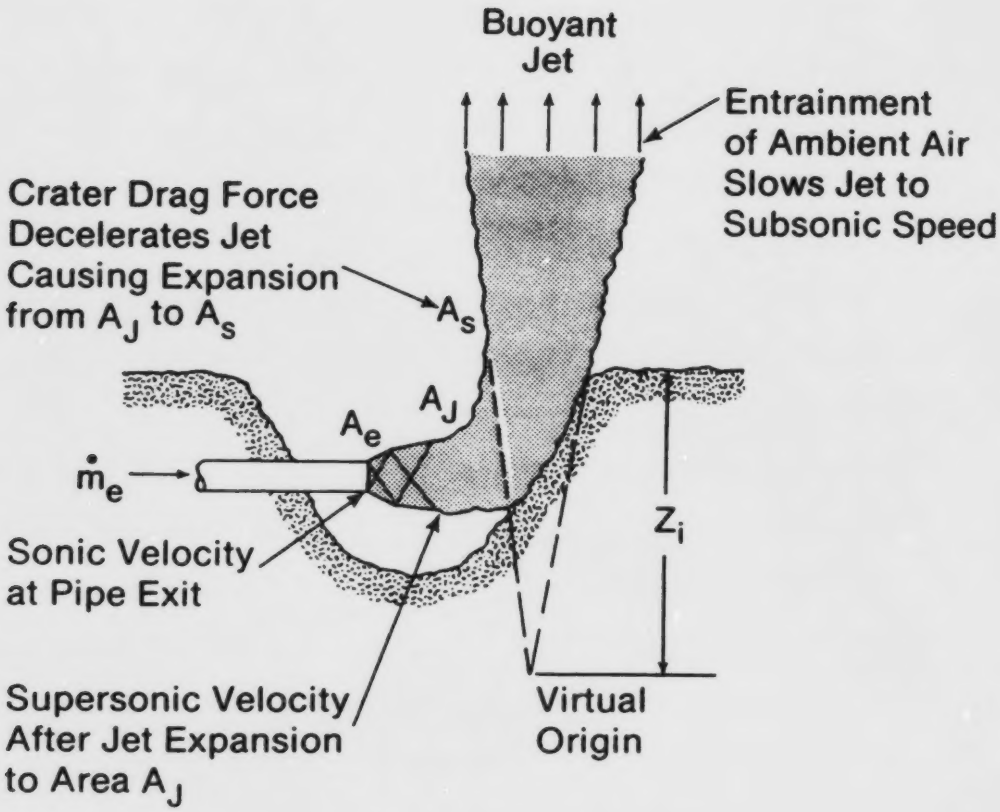

Figure 3-1 Jet Expansion Outside the Pipe

Including the Effect of Turbulence Kinetic Energy

The conventional form of the first law of thermodynamics for adiabatic flow assumes that all of the kinetic energy is contained in mean flow, with no turbulence. In most situations this is a reasonable approximation, because turbulent energy in pipe flows seldom exceeds 1% of the mean kinetic energy. This will not be the case for the highly turbulent mixing region outside the pipe rupture.

In the mixing zone of the rupture jet the turbulence kinetic energy may be as high as 100% of the mean kinetic energy, and even higher in reverse flow regions. The total stagnation enthalpy $C_p T_o$ remains constant in an adiabatic flow and is distributed between internal thermal energy, mean kinetic energy, and turbulent kinetic energy in the form

$$C_p T_o = C_p T + \frac{V^2}{2} + \frac{\overline{V'^2}}{2} \tag{3-1}$$

where T_o = stagnation temperature

T = static fluid temperature

C_p = constant pressure specific heat

$\frac{V^2}{2}$ = mean kinetic energy

$\frac{\overline{V'^2}}{2} = \frac{\overline{u^2} + \overline{v^2} + \overline{w^2}}{2}$ = turbulence kinetic energy

Using the turbulence intensity i_v defined by

$$i_v^2 = \frac{\overline{V'^2}}{V^2} \tag{3-2}$$

The mass flow at any point in an adiabatic process of an ideal gas may be written (see Shapiro (1953) p. 82)

$$\frac{\dot{m}}{A} = \frac{P}{\sqrt{T_o}} \cdot \left[\frac{M^2 k}{R} \left(1 + \frac{k-1}{2} (1 + i_v^2) M^2 \right) \right]^{0.5} \tag{3-3}$$

where $\dot{m}$ = mass flow rate kg/sec

A = flow area m^2

P = static pressure N/m^2

T_o = stagnation temperature ^oK

M = local Mach number

k = specific heat ratio

R = gas constant $N\text{-}m/kg^oK$

Using (3-3) a ratio can be formed between the pipe exit point "e" and the source "s." It will be assumed that $i_v = 0$ in the jet at the exit. Noting that $M_e = 1.0$ the ratio is

$$\frac{A_s P_a}{A_e P_e} = \left[\frac{\frac{k+1}{2}}{M_s^2 \left(1 + \frac{(k-1)}{2} (1 + i_{vs}) M_s^2 \right)} \right]^{0.5} \tag{3-4}$$

The velocity of the jet at the source location is computed by first evaluating the source temperature T_s from

$$\frac{T_{oe}}{T_s} = 1 + \frac{(k-1)}{2} (1 + i_{vs}^2) M_s^2 \tag{3-5}$$

and using T_s to compute the local sonic speed at "s,"

$$C_s = \sqrt{kRT} \tag{3-6}$$

from which the velocity at the source is

$$W_s = C_s M_s \tag{3-7}$$

If it can be shown that for typical pipeline ruptures the velocity at the source W_s is almost completely insensitive to the choice made for the source turbulence kinetic energy. It is suggested that the value $i_{vs} = 1.0$ be used for all cases.

Choosing the Source Exit Area A_s

In the preceeding analysis it is necessary to specify the source area A_s of the jet after expansion and mixing processes are complete. Because the interaction between the compressible jet and the sides of the hole created by the rupture are difficult to determine in advance, the selection of A_s is rather arbitrary. As an upper limit the source area may be specified as the ground level area created by the hole caused by the pipe rupture. This is typically 5 to 10 square meters.

However, the situation shown in Figure 3-1 is probably more typical, with the jet from the source occupying only a small fraction of the total ground level hole area. Based on observations of actual pipeline ruptures during the recent field test program at Pincher Creek, a lower limit on this source area is expected to be about 1 square meter.

It is more relevant to ask what effect the choice of source area will have on plume rise and dispersion. The buoyancy flux used to compute buoyant plume rise is independent of source area, and is governed only by the total mass release rate. In contrast, the momentum flux F_m of a jet is inversely proportional to A_s^2. Because final momentum rise is directly proportional to $F_m^{0.5}$, the momentum rise will depend inversely on A_s. For plumes where momentum dominates buoyancy effects, a reasonable estimate must be made for A_s to accurately determine plume rise.

Incompressible Approximation for Source Velocity

Based on the previous discussion we expect that the source area will lie somewhere in the range of $1 < A_s < 10 m^2$ (or approximately $1 < D_s < 3m$). When the exact incompressible relations in equations 3-4 to 3-7 are used to compute the source conditions for relatively large release rates of about

100 kg/s, and with the smallest reasonable source diameter D_s = 1m, the source temperature is found to be almost equal to the stagnation temperature at the pipe exit. This is shown schematically on the temperature-entropy diagram in Figure 3-1. This result suggests that a simple incompressible flow approximation may be made to the jet at the source location. In this approximate analysis it is assumed that the Mach number at the source M_s is small enough that the source temperature is the same as the pipe temperature (see equation 3-5). With this approximation the velocity at the source may be evaluated directly from the release rate $\dot{m}_e$

$$\dot{m}_e = \rho_s A_s W_s \tag{3-8}$$

using $\rho = P/RT$ with $P_s = P_a$ and $T_s \cong T_{oe}$

$$W_s \cong \frac{\dot{m}_e R T_{oe}}{P_a A_s} \tag{3-9}$$

Equation 3-5 will be within 5% of the exact compressible flow result if

$$W_s < 0.4 \sqrt{kRT_{oe}} \tag{3-10}$$

This approximate method allows us to compute the momentum flux F_m directly from the definition

$$F_m \cong \frac{\rho_s}{\rho_a} W_s^2 r_s^2 \tag{3-11}$$

where r_s is the source radius.

$$F_m = \frac{\dot{m}_e^2}{\rho_s \rho_a \pi A_s} \tag{3-12}$$

which, as discussed previously, is inversely proportional to A_s.

The buoyancy flux F can also be readily computed from its definition

$$F = g\left(\frac{\rho_a - \rho_s}{\rho_a}\right) W_s r_s^2 \tag{3-13}$$

or

$$F = g\left(\frac{\rho_a - \rho_s}{\rho_s \rho_a}\right) \frac{\dot{m}_e}{\pi} \tag{3-14}$$

which is independent of A_s.

Both the momentum flux F_m and the buoyancy flux F require the source density for their evaluation. For the approximation that the source temperature and the exit stagnation temperature are the same, the source density is given by

$$\rho_s \cong \frac{P_a \tilde{M}_e}{\bar{R}\, T_{oe}} \tag{3-15}$$

where P_a = ambient pressure N/m^2

$\tilde{M}_e$ = molecular weight of the gas in the pipe

$\bar{R}$ = 8310 N-m/kg mol ^oK, the universal gas constant

T_{oe} = stagnation temperature at the pipe exit, ^oK

also

$$\rho_a = \frac{P_a M_a}{\bar{R}\, T_a} \tag{3-16}$$

where M_a, P_a and T_a are the molecular weight, pressure and temperature of the ambient air.

Finally, it should be kept in mind that the stagnation temperature T_{oe} may vary with time. At any given instant, the stagnation temperature is constant along the length of the flow inside the pipe, and in the mixing region outside. However, due to the adiabatic expansion of the gas inside the pipe with time, the stagnation temperature at the pipe exit may gradually decrease as the pipe mass flow depletes. Recent experiments

using full scale ruptures at Pincher Creek, Alberta have found heat transfer from the pipe walls makes the depletion process almost isothermal, with T_{oe} constant with time.

Numerical Example

To demonstrate how the equations in this section can be applied to determine source conditions, consider the following numerical example:

Mass release rate $\dot{m}_e = 100$ kg/s

pipe diameter = 6", $A_e = 0.0182\ m^2$

pipeline gas $k = 1.25$, $M_e = 25$

source diameter = 1.0m, $A_s = 0.786\ m^2$

source turbulence intensity, $i_v = 1.0$

stagnation temperature at pipe exit, $T_{oe} = 250^oK$

ambient barometric pressure $P_a = 10^5\ N/m^2$

The gas constant for the pipeline gas is

$$R = \frac{\bar{R}}{M_e} = \frac{8310}{25} = 332\ Nm/kg^oK$$

Compute the exit pressure from (3-3) at the pipe exit where $M_e = 1.0$, $i_v = 0$

$$\frac{\dot{m}_e}{A_e} = \frac{P_e}{\sqrt{T_{oe}}}\left[\frac{k}{R}\left(\frac{k+1}{2}\right)\right]^{0.5}$$

$$\frac{100}{0.0182} = \frac{P_e}{\sqrt{250}}\left[\frac{1.25}{332}\left(\frac{1.25+1}{2}\right)\right]^{0.5}$$

$$P_e = 13.3 \times 10^5\ N/m2$$

Using (3-4)

$$\frac{0.786}{0.0182} = \frac{13.3 \times 10^5}{10^5}\left[\frac{\frac{1.25+1}{2}}{\frac{M_s^2}{1 + 0.25\ M_s^2}}\right]^{0.5}$$

$$M_s^2 = \frac{0.1067}{1 + 0.25\ M_s^2}$$

Carrying out an iterative solution, $M_s = 0.332$. Using (3-5) $T_s = 243^oK$, (compared to $T_{oe} = 250^oK$). The sonic speed at the source is using (3-6)

$$C_s = \sqrt{1.25\ (332)(243)} = 318\ m/s$$

From which (3-7) gives

$$W_s = 318\ (0.322) = 102.6\ m/s$$

Using the approximate method (3-9) predicts

$$W_s = \frac{100\ (332)(250)}{10^5\ (0.786)} = 105.6\ m/s$$

which is close to the exact value of 102.6 because, from (3-10)

$$W_s < 0.4\sqrt{1.25\ (332)(250)}$$

$$W_s < 129\ m/s$$

SECTION 4
GAUSSIAN PLUME MODEL WITH DOWNWIND DIFFUSION OF SOURCE TRANSIENTS

By comparison with a direct integration of the differential equation of mass diffusion using empirical diffusivities, the Gaussian plume or puff model is much simpler to use, and has inaccuracies which are no greater than the uncertainties inherent in empirical diffusion coefficients themselves. For a plume with a continuous and steady rate of release, the Gaussian plume equation is the standard used for determining ground level concentrations. Unfortunately, the continuous plume equation is derived by ignoring diffusion in the windward direction, and thus contains no along-wind spreading coefficient σ_x. The reason why σ_x does not appear in the continuous plume equation, is that diffusion in the along-wind direction simply redistributes the constant mass release rate to different x locations, with no net change in the mass flux passing over a given point. For a source release rate which varies with time, the along-wind diffusion, characterized by the spreading rate σ_x, will tend to smear out any x direction variation in the instantaneous mass flow rate. In order to account for the effect of along-wind diffusion, there are two existing techniques:

1. The integrated puff model subdivides the time-varying release into a series of individual puffs which have the capability of spreading in all three directions x, y, and z. The difficulty with this model is that it requires considerable computer time to provide the puff superposition Because a numerical solution is required, little insight can be gained into the mechanisms governing the diffusion process.

2. The plume segment model divides the time-varying plume into a series of lengthwise segments each of which has its mass flow averaged over the time of release. By suitably choosing the length of each segment, the along-wind diffusion is provided by this averaging process. Lott(1977) describes one method for selecting these segment lengths. Because of the rapid transient variation of mass release rate with time, the short segment lengths required to simulate a pipeline rupture would virtually reduce the plume segment model to an integrated puff model. The plume segment model is best suited for use in situations where the source release rate varies only slowly with time, in which case both source variations and changes in wind speed and direction can be included. The plume segment model is not suitable for the rapid release rates characteristic of pipeline ruptures.

The Effect of Along-Wind Diffusion on a Plume

In the absence of any along-wind diffusion the mass release rate will be "frozen" into the flow as it passes over the point of release. This frozen mass release rate will be carried in the x direction by the wind speed U until it passes over a receptor point. At any given time t the concentration at ground level will be determined only by the frozen mass release rate that is passing at that moment directly above the receptor point.

However, when the effects of x direction diffusion are included, the mass rate being convected above a point will no longer be the frozen value, but rather some average from mass that has convected upwind and downwind and now lies over the location in question. This is shown schematically

in the sketch below.

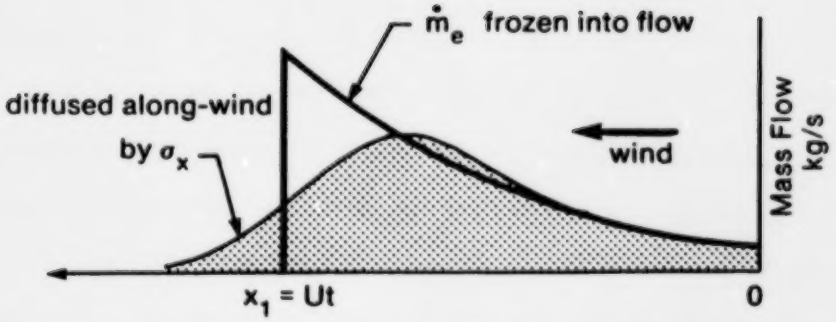

The contribution to the mass flux above a location x_1 is simply the Gaussian diffusion in the x direction from all locations upwind and downwind of that point. The contribution from a location x_2 is shown in the sketch below.

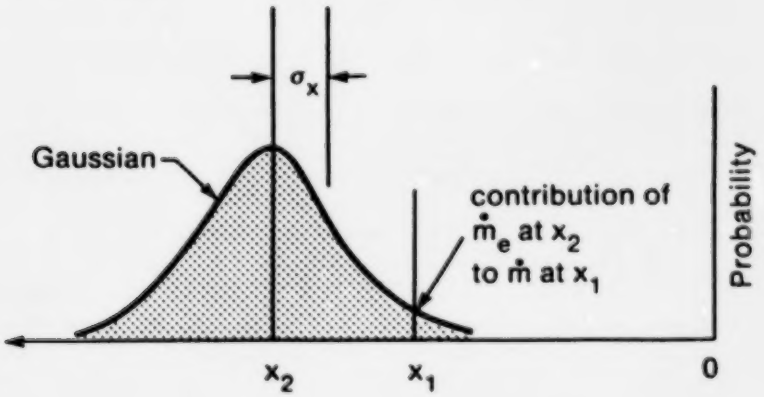

The greatest obstacle to simply integrating all these contributions to determine the effective mass flux passing above location x_1 is that the spreading rate σ_x is also a function of x, making a closed form integration difficult. It is this dependence of σ_x on x that makes a numerical solution of the integrated puff model necessary.

Approximations for x Direction Diffusion

In order to obtain closed-form solutions for the contribution of along-wind diffusion to the effective mass flux above a receptor, only two simple approximations are necessary.

1. At any specified location x_1 assume that the contribution to the effective mass flow above x_1 can be computed using the spreading rate σ_{x1}. This assumption makes σ_x a constant in the subsequent integration used to find the mean effective mass flux above x_1.
2. For all x positions which contribute significantly to the effective mass flux above position x_1, it is assumed that the plume centerline is at a constant elevation above ground level.

How reasonable are these assumptions? Because 95% of the contributions to mass flow above a point x_1 will come from $\pm 2\sigma_{x1}$ upwind and downwind of x_1, the assumption of a constant value for σ_{x1} will be justified if

$$2\sigma_{x1} \frac{d\sigma_x}{dx} << \sigma_{x1} \qquad (4\text{-}1)$$

as shown in the diagram in Figure 4-1. Taking as an approximation in neutral stability that $\sigma_x \simeq 3\sigma_z$ and that $\sigma_z = 0.2\ x^{0.76}$, for measurements in meters, (4-1) becomes

$$\frac{d\sigma_x}{dx} << \frac{1}{2}$$

$$0.46x^{-0.24} << \frac{1}{2}$$

At x = 200 meters the inequality is 0.13 << 0.5, which may be reasonable.

The assumption of constant source height over $\pm 2\sigma_{x1}$ requires that, for a plume centerline height "h" above ground

$$2\ \sigma_{x1} \frac{dh}{dx} << h \qquad (4\text{-}2)$$

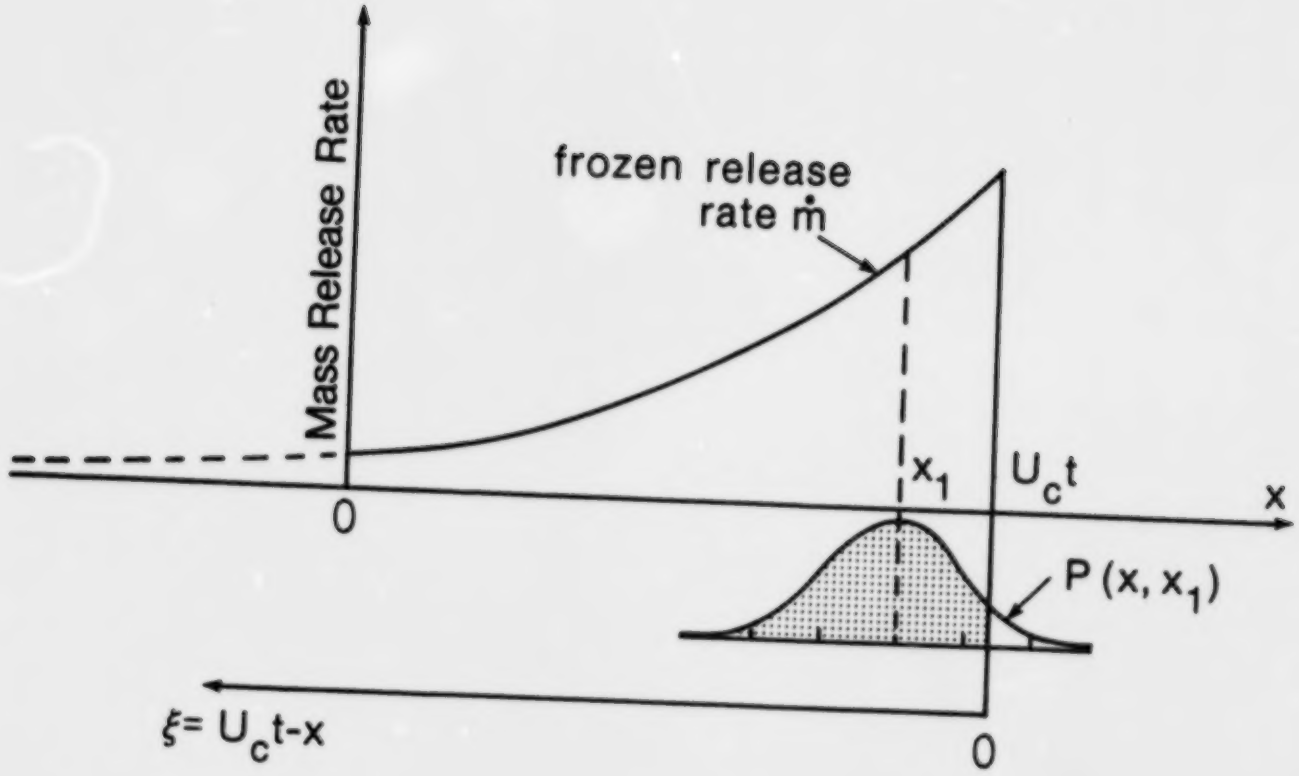

Figure 4-1 Varying Mass Flow Rate Frozen into the Passing Flow

For a momentum dominated plume $h \propto x^{1/3}$ so that

$$\frac{dh}{dx} = \frac{h}{3x}$$

and (4-2) becomes

$$\sigma_{x1} << \frac{3}{2} x$$

At x = 200 m the inequality is 33 << 300 which is certainly reasonable.

When the validity of the two approximations above are weighed against the advantages of obtaining simple closed form solutions, it was concluded that the assumptions were reasonable, considering other uncertainties in the diffusion problem.

Effective Plume Model

Figure 4-1 shows a transient release rate typical of pipeline ruptures. The system is shown a time t after release, where the frozen mass flow distribution has been convected downwind distance Ut. The contribution to the diffusion averaged mean mass flow $\bar{m}_{is}$ given for a t after release as,

$$\bar{m}(x_1,t) = \int_{x=-\infty}^{x=Ut} \frac{\dot{m}_e}{\sqrt{2\pi}\,\sigma_{x1}} \exp\left[-\frac{(x_1-x)^2}{2\sigma_{x1}^2}\right] dx \qquad (4\text{-}3)$$

where $\dot{m}_e = \dot{m}_e\left(t - \frac{x}{U}\right)$, see Figure 4-1

The upper limit of the integral has been set at x = Ut rather than $x = +\infty$ because $\dot{m}_e = 0$ for x > Ut. The lower limit has been extended to $x = -\infty$ as an aid in obtaining simple closed form solutions. Because the release rate $\dot{m}_e$ further than $\pm 2\,\sigma_{x1}$ on either side of a point x_1 has virtually no influence on $\bar{m}$, defining $\dot{m}_e$ for x < 0 is simply a

mathematical convenience .

The Gaussian diffusion equation for ground level concentration from an elevated source is then

$$c(x_1,t) = \frac{\bar{m}(x_1,t)}{\pi U \sigma_y \sigma_z} \exp \left[- \frac{h^2}{2\sigma_z^2} - \frac{y^2}{2\sigma_y^2} \right] \qquad (4\text{-}4)$$

It can be easily shown, that for a steady continuous source with a constant mass release rate, equation 4-3 is $\bar{m}$ = const. and 4-4 becomes the usual continuous plume diffusion equation. For an instantaneous release at t = 0, using dx = Udt and $\dot{m}_e dt = m_I$ = const. the combination of 4-3 and 4-4 is simply the instantaneous puff equation with ground level reflection. Thus, the effective plume model given by 4-3 and 4-4 show the proper functional forms in their limiting cases.

Effective Source Strength $\bar{m}$ for Exponential Release Rate

The release rate for many real processes can be accurately approximated by an exponential, or a series of exponentials. Because a series of exponentials can be integrated term by term, it is only necessary to consider a release rate in the form of a single exponential

$$\dot{m}_e = \dot{m}_{oe} \exp(-t/\tau) \qquad (4\text{-}5)$$

where $\dot{m}_{oe}$ is the inital release rate at t = 0 and τ is the time constant. At $t = \tau$, 63.2% of the total mass will have been released. Inserting (4-5) in (4-3) the integral can be evaluated after transforming to ζ coordinates (see Figure 4-1). The value of the resulting exponential - Gaussian integral is given by Geronimus and Tseytlin (1965) and by Abramovitz and Stegun (1965) as

$$\bar{m}\,(x_1,t) = \frac{\dot{m}_e(t_1)}{2}\ \exp\left(\frac{\sigma_{x1}^{\,2}}{2U^2\tau^2}\right)\left[1 - \text{erf}\,(\gamma)\right] \qquad (4\text{-}6)$$

where $$\gamma = \frac{\sigma_{x1}}{\sqrt{2}\,U\tau} - \frac{(Ut-x_1)}{\sqrt{2}\,\sigma_{x1}}$$

and $\dot{m}_e(t_1)$ is the "frozen" release rate that lies above x_1,

$$\dot{m}_e(t_1) = \dot{m}_{oe}\ \exp\left[\frac{-\left[t - \frac{x_1}{U}\right]}{\tau}\right] \qquad (4\text{-}7)$$

The error function erf(γ) is tabulated in Abramovitz and Stegun (1965) and is defined as

$$\text{erf}\,(\gamma) = \frac{2}{\sqrt{\pi}} \int_0^{\gamma} \exp\,(-\phi^2)\,d\phi \qquad (4\text{-}8)$$

which has the property that erf($-\gamma$) = $-$erf(γ), necessary to evaluate the it for negative arguments.

Numerical Example

The diffusion averaged effective source strength given by equation 4-6 is simple enough to evaluate by hand calculation. A numerical example was carried out for release into a neutrally stable atmosphere with the

following source and meteorological parameters

Release rate time constant τ = 50 s

Effective wind speed U = 5 m/s

Time after release t = 100 and 200 s

The value of σ_x was taken for neutrally stable conditions, Z_o = 100 cm, including the effect of vertical windshear

$$\sigma_x^2 = 4.89 \times 10^{-5} x^3 + 0.12 x^{1.52}$$

The constants in this relation are for a 0.2 velocity power law, with a critical height of 10 meters used to evaluate vertical wind shear. The general form for σ_x is developed in Section 7 of this report.

Figure 4-2 shows the diffusion averaged effective source strength computed using the above conditions. It is apparent that x direction diffusion causes a considerable reduction in the maximum effective source strength above points near the leading edge of the plume.

The results of this numerical example can also be used to determine the spacing of isopleths for a ground level release. For a ground level release the maximum concentration at a given downwind location occurs when the peak value of the effective source strength passes over the receptor. Concentration along the center line of a ground level source may be derived from equation 4-4 as

$$c_{max} = \frac{\bar{m}_{max}}{\pi U \sigma_y \sigma_z}$$

For neutral stability with a surface roughness Z_o = 10 cm it will be shown in Section 7 that

$$\sigma_y \propto x^{0.88}$$

$$\sigma_z \propto x^{0.76}$$

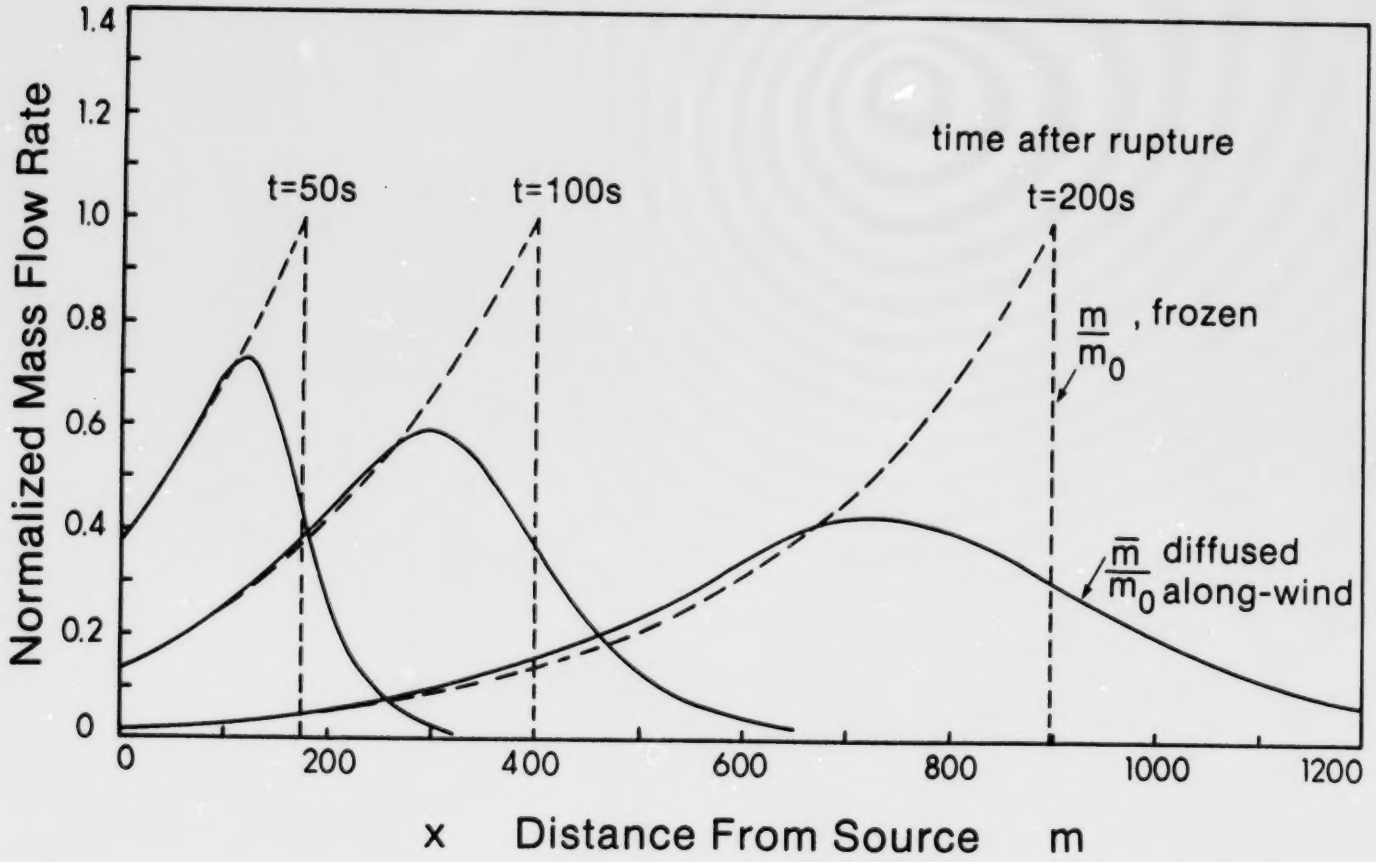

Figure 4-2 Comparison of Frozen and Along-Wind Diffused Mass Flux Distributions

For the 3 profiles of $\bar{m}$ shown in Figure 4-2, it can be deduced that

$$\bar{m}_{max} \propto x^{-0.61}$$

Combining these equations yields

$$c_{max} \propto x^{-2.25}$$

This shows that the spacing between values of maximum observed ground level concentration is nonlinear. If the 500 ppm maximum concentration point is located at x = 1500 m, the 1000 ppm point will occur at x = 1100 m and the 250 ppm point at x = 2040 m. From this it may be inferred that large errors in specifying the allowable toxic concentration will not have much effect on the "safe" distance from the rupture. (It must be kept in mind that this simple example neglects plume rise, concentration fluctuations and other important factors in risk analysis)

This last proportionality shows that the location of a specified critical concentration is not very sensitive to errors in the concentration. For example if 500 ppm of H_2S was assumed to be the critical concentration for a fatal dose; if subsequent calculations showed that this occurred x = 1500 m, a change in the estimated fatal concentration to 1000 ppm would only move the location to x = 1100 m.

SECTION 5
STANDARD METEOROLOGICAL CONDITIONS FOR DISPERSION ANALYSIS OF PIPELINE RUPTURES

Previous analytical methods for evaluating dispersion from pipeline ruptures have focussed on the "worst case" conditions, that of a stable atmosphere with a low mean wind speed. This approach is not correct in carrying out a risk analysis, because by its nature the risk calculation must consider all probable meteorological conditions, including those which rapidly disperse the gas released from the rupture. A complete risk analysis would be forced to consider a very large number of combinations of atmospheric stability and wind speed to determine the probability of exceeding a specified concentration level at a given downwind location.

In addition to the variables of wind speed in an atmospheric stability, each site location has a characteristic terrain surface roughness Z_o which influences the atmospheric turbulence level, and hence the spreading rate of the plume. Each site may also be subject to its own special collection of terrain irregularities such as hills, valleys, and sudden changes in surface roughness between open fields and forested areas.

All of the above factors cannot be considered if the risk analysis is to be carried out with a reasonable expenditure of time and effort. It is suggested that the minimum number of different meteorological conditions that must be considered are:

1. Three different stability classes, unstable, neutral, and stable.
2. A single typical wind speed for each of the three stability classes.
3. Two different terrain roughness heights, open fields typical of agricultural areas, and heavily wooded regions typical of forests and

mountain foothills.

Each specific site would be categorized as having one of the two surface roughness levels, and its meteorological data base would be used to establish the fraction of time that each of the three stability and wind conditions prevail. The most restrictive of all the above assumptions is the specification of only a single "typical" wind speed for each of the three stability classes. If a more realistic model of the varying meteorological conditions was required, the most logical extension of the above system would be to specify an additional wind speed for each of the stability categories.

Surface Roughness and Wind Speed Power Law

Fortunately, the wind speed and atmospheric turbulence change only gradually with large changes in terrain roughness. It would appear to be reasonable to assign all of the terrain to one of two roughness categories, Z_o = 10 cm and Z_o = 100 cm. The smallest value of terrain surface roughness is typical of open fields in agricultural areas, while the larger roughness value is typical of urban areas and heavily forested regions.

The surface roughness specification Z_o arises directly from the logarithmic law of velocity variation with height in a neutrally stable atmosphere. The wind speed may also be specified by a power law in the form

$$\frac{U}{U_{ref}} = \left[\frac{Z}{Z_{ref}}\right]^n \qquad (5\text{-}1)$$

The power n can be adjusted to describe various surface roughness conditions, as well as variations in atmospheric stability. The velocity power law can be directly related to the surface roughness by matching the

slopes of the logarithmic and power law profiles at any specified height above ground Z_{ref}

$$n = \frac{1}{\ln \frac{Z_{ref}}{Z_o}} \qquad (5\text{-}2)$$

Taking the reference height as Z_{ref} = 10 m, the power law for neutral stability should be n = 0.217 for Z_o = 10 cm and n = 0.434 for Z = 100 cm.

The three dispersion classes chosen for pipeline rupture analysis will be Pasquill classes B, D, and F. Touma (1977) examined the variation of wind speed power law with atmospheric stability in the range from 10 to 60 meters above ground level. His results, corrected for variations in terrain roughness Z_o and evaluated at a reference height Z_{ref} of 10 meters give the following recommended values for the various stability and roughness conditions.

Table 5-1

Wind Speed Power Law "n" at Z_{ref} = 10 m

Stability	Pasquill Class	n	
		Z_o = 10 cm	Z_o = 100 cm
Moderately Unstable	B	0.20	0.40
Neutral	D	0.20	0.40
Moderately Stable	F	0.40	0.50

The upper limit of power law of 0.50 for stable conditions is consistent with the wind tunnel results of Chuang and Cermak (1969), who found that the power law never exceeded a value of 0.55 even under very stable conditions.

Selecting Mean Wind Speed U

A considerable amount of subjective judgement is required here if a large number of wind speeds, with an excessive number of calculations is to be avoided. The only constraint is that the "typical" values must be selected consistent with the Pasquill stability classes, and with typical Alberta values. Using the stability chart developed by Smith, (see Pasquill (1975) p 374) the following average values are suggested.

Table 5-2

"Typical" Wind Speeds for Pasquill Stability Classes

Stability	Pasquill Class	U_{10} @ Z = 10 m m/s	
		range	"typical"
Moderately Unstable	B	2 to 5	3
Neutral	D	> 4	5
Moderately Stable	F	2 to 3	2

Potential Temperature Gradients

Fortunately, the use of Pasquill stability classes to specify the atmospheric conditions implies a specific set of plume spreading rates for each stability class. However, to evaluate plume rise under stable conditions it is necessary to know the stability factor S, which is related to the potential temperature gradient in the form

$$S = \frac{g}{T} \frac{d\theta}{dz} \qquad (5\text{-}3)$$

A correlation of atmospheric stability data by Luna and Church (1971) and by Golder (1972) indicates that it is the Richardson number that is more

likely to remain constant for a given stability class than the stability factor S. For a power law velocity profile the Richardson number at a height of Z = 10 meters is defined as

$$Ri = \frac{S}{\left(\frac{dU}{dz}\right)^2}$$

$$Ri_{10} = \frac{S}{\left(\frac{n\, U_{10}}{10}\right)^2} \qquad (5\text{-}4)$$

Using the experimental data of Touma (1977), as well as the experimental correlations of Luna and Church (1971), and Golder (1972), it was found that the average Richardson number at 10 meters for class F stability was about $Ri_{10} \tilde{=} 0.10$ at Z_o = 10 cm and $Ri_{10} \tilde{=} 0.06$ for Z_o = 100 cm. The lower value of Richardson number for the high surface roughness indicates that the turbulence generated near the ground by surface roughness acts to mix the flow near the ground and reduce vertical temperature gradients.

Because very strong inversions due to radiational cooling at night are typical in Alberta, it is suggested that Richardson numbers about twice these average values be used. The recommended values are

Table 5-3

Richardson Numbers and Potential Temperature Gradient

Stability	Pasquill Class	Ri_{10} @ Z = 10 m	
		Z_o = 10 cm	Z_o = 100 cm
Moderately Unstable	B	-	-
Neutral	D	0	0
Moderately Stable	F	0.20	0.10

At a temperature of $0^{o}C$, using the definition of Ri_{10}, these values imply potential temperature gradients of $3.5^{o}C/100$ m for Z_o = 10 cm and $2.8^{o}C/100$ m for Z_o = 100 cm, both for U_{10} = 2 m/s.

Effective Wind Speed for Diffusion

The diffusion plume from a ground level release spreads upward and in doing so sees successively higher velocities due to vertical wind shear. The mean wind speed at which the plume is convected downwind must be some suitable averaged value. This average convective speed will increase with downwind distance as the plume spreads upward and samples higher and higher velocities.

Hogstrom (1964) p 236 develops an expression for the effective convective velocity by carrying out a mass balance upon the plume passing a given location. He considers only the case of a ground level release. For an elevated release the integration becomes much more complicated, and requires the additional specification of source height in order to obtain a solution. For a ground level source where h = 0, the effective velocity U for use in the plume equation 4-4 was given by

$$U = \frac{U_{ref}}{\sqrt{2\pi}\,\sigma_z} \int_0^{\infty} \left(\frac{Z}{Z_{ref}}\right)^n \exp\left[\frac{-Z^2}{2\sigma_z^2}\right] dz \qquad (5\text{-}5)$$

which reduces to $U = U_{ref}$ when n = 0. Because this formulation requires a numerical integration, and in any case is only valid for ground level releases, a more simple approach is suggested. For a ground level release with plume rise, it is suggested that the convective speed be evaluated at the average of the source height plus plume spread σ_z to give,

$$U = U_{ref}\left[\frac{\Delta h + \sigma_z}{2\,Z_{ref}}\right]^n \qquad (5\text{-}6)$$

In many cases the plume rise is unknown, although it may be significant. Under these conditions, it is suggested that a constant convection speed equal to the wind speed at 10 meters height be used.

SECTION 6
PLUME RISE FROM A GROUND LEVEL SOURCE

As the gas accelerates to sonic velocity at the pipe exit, its temperature rapidly drops as its internal thermal energy is converted to kinetic energy. Outside the rupture the jet expands to come into equilibrium with the local ambient pressure. During this expansion process the diameter of the jet increases, and its velocity is drastically reduced. This reduction in velocity converts the kinetic energy back to internal thermal energy, causing the jet temperature to return to the stagnation temperature, which is the temperature of the gas in the pipe before rupture. This mixing process is described in detail in Section 3 of this report.

The density of gas in the jet at the source will be somewhat less than the surrounding air density because the pipeline is usually operated at temperatures exceeding the surrounding ambient temperature, and at the same time the molecular weight of the pipeline gas is always less than that of air. The gas jet from the rupture will experience both momentum and buoyancy forces and the plume rise will be a combination of these effects. The combined rise due to momentum and buoyancy has been derived by Slawson (1978) and others. It can be shown to have the form

$$\Delta h = \left[\Delta h_M^3 + \Delta h_B^3 + \left(\frac{r_o}{\beta}\right)^3 \right]^{1/3} - \frac{r_o}{\beta} \qquad (6\text{-}1)$$

where

$$\Delta h_M^3 = \frac{3}{\beta^2} \frac{F_m x}{U^2} \qquad (6\text{-}2)$$

$$\Delta h_B^3 = \frac{3}{2\beta^2} \frac{F x^2}{U^3} \qquad (6\text{-}3)$$

Δh = combined plume rise, m

Δh_M = momentum rise, m

Δh_B = buoyancy rise, m

r_o = initial plume radius, m

β = entrainment constant, typically β = 0.6 to 0.9

x = distance from the source, m

U = effective windspeed, m/s

F_m = jet momentum flux, see eq. 3-11 m^4/s^2

F = jet buoyancy flux, see eq. 3-13 m^4/s^3

Because the combined rise depends on the sum of cubes of various terms, one term always becomes dominant, and the plume rise can usually be approximated by either the momentum or buoyancy rise. The initial source radius r_o is usually not significant for most practical problems.

Because the buoyancy rise has the form $\Delta h_B^3 \propto x^2$ while the momentum rise varies as $\Delta h_M^3 \propto x$ the buoyancy term will eventually dominate the combined plume rise.

Final Buoyancy and Momentum Rise

The buoyancy effects will only succeed in dominating momentum if the plume continues to rise indefinitely with downwind distance. In fact, atmospheric turbulence eventually causes the plume to break up and terminate its rise. Briggs (1975) has examined this problem and determined equations for final rise. The key assumption in his analysis is that the plume will terminate its rise when the rate of turbulence energy dissipation in the plume itself is equal to the energy dissipation rate of the atmospheric turbulence being entrained into the plume. By choosing the rate of turbulence energy dissipation rather than the intensity of turbulence as the criteria for plume break-up, only the smallest size range of turbulence

eddies are considered. This is a reasonable assumption because the large-scale atmospheric turbulence, which does not contribute much to turbulence energy dissipation, should act only to cause the plume to meander and not to cause plume break-up.

Because the atmospheric turbulence is the factor which causes plume rise to terminate, the final rise height should be considerably smaller for a ground level source which sees a much larger proportion of small eddy turbulence than for a source from a high stack where atmospheric dissipation rates are much smaller.

Briggs (1975), p 89 derives equations for final rise of buoyant plumes and momentum jets. If the atmospheric turbulence and mean convective wind speed are evaluated at a fixed height above ground, the final rise equations for a ground level release can be written as

$$\Delta h_{Bf} = \gamma_B \frac{F}{U_{10}^3} \tag{6-4}$$

$$\Delta h_{Mf} = \gamma_M \left(\frac{\rho_s}{\rho_a}\right)^{1/2} \frac{W_s}{U_{10}} r_s \tag{6-5}$$

Δh_{Bf} = final buoyancy rise, m

Δh_{Mf} = final momentum rise, m

γ_B and γ_M = final rise constants

ρ_s = gas density at the source kg/m^3

ρ_a = ambient density, kg/m^3

W_s = vertical velocity at the source, m/s

r_s = jet radius at the source, m

U_{10} = wind speed at z = 10 m, m/s

Using an entrainment constant of $\beta = 0.6$ and evaluating the turbulence dissipation rate and mean convective windspeed at $z = 20$ m the final rise constants γ_B and γ_M were evaluated for conditions of neutral stability. They are summarized in Table 6-1, where the rise constants for the moderately unstable atmosphere are assumed to be the same as for neutral stability. The justification for using the same plume rise in both unstable and neutrally stable conditions is that the small scale turbulence which is responsible for the energy dissipation rate and therefore for the termination of rise, should be the same in both cases.

Final Rise in Stable Conditions

Under stable atmospheric conditions the effective buoyancy decreases as the plume rises, until it eventually terminates its rise at the location where the effective plume buoyancy has decreased to zero. Briggs (1975) gives this location for elevated stacks as

$$\Delta h_{Bf} \cong 2.6 \left(\frac{F}{US}\right)^{1/3} \qquad (6\text{-}6)$$

For a given Pasquill stability class, in this case class F, it is the Richardson number defined by equation 5-4 and not the non-dimensional temperature gradient S that remains constant for varying wind speeds. Using a power law velocity profile the Richardson number at any height z is given by

$$Ri_z = \frac{S}{\left(\frac{nU_z}{z}\right)^2}$$

Combining this with equation 6-6 and evaluating the Richardson number at the plume height reduces the equation to

TABLE 6-1

FINAL RISE CONSTANTS FOR BUOYANT

PLUMES AND MOMENTUM JETS

Stability	Pasquill Class	Surface Roughness Z_o	Buoyancy γ_B	Momentum γ_M
Moderately Unstable	B	10 cm 100 cm	150 50	5 3
Neutral	D	10 cm 100 cm	150 50	5 3
Moderately Stable	F	10 cm 100 cm	110 150	6 4

$$\Delta h_{Bf} = \frac{17.6}{n^2 Ri_{10}\left(\frac{z}{10}\right)^{2+n}} \frac{F}{U_{10}^3} \qquad (6\text{-}7)$$

Taking $z \simeq 20$ m for the plume rise, to be consistant with the neutrally stable case, and using the Richardson numbers from Table 5-3, the final rise can be computed from equation 6-7. Because 6-7 has exactly the same form as 6-4, these constants are tabulated in Table 6-1 for use in equation 6-4.

Downwind Location of Final Rise

By inserting the final rise equations 6-4 and 6-5 in the transitional rise formulas 6-2 and 6-3, the downwind position where plume rise terminates can be computed. It is found that for a buoyant plume final rise position is

$$x_{Bf} = \frac{\gamma_B}{2.02} \cdot \Delta h_{Bf} \qquad (6\text{-}8)$$

And for a momentum jet, the location of final rise occurs at

$$x_{Mf} = \frac{\gamma_M^2}{8.33} \Delta h_{Mf} \qquad (6\text{-}9)$$

Flow Rate for Plume Rise Analysis

All of the preceding plume rise equations are strictly valid only for a steady constant flow rate from the source. For the case of a pipe rupture the rate of mass release varies rapidly with time, and some adjustment of the plume rise must be made to account for this.

For the purposes of calculating plume rise it is tempting to use the x direction diffusion averaged mass flux $\bar{m}$, computed from equation 4-3. However, it must be recognized that this is at best only an approximation,

because the plume rise represents an integrated process which occurs from the point of release to the given downwind position. This means that the plume rise at any fixed x location will depend on the time history of the plume segment, and not just on the average mass flux above that position.

If we take the final maximum rise expected for pipeline ruptures as about 50 meters, equations 6-8 and 6-9 show that the final rise for buoyancy and momentum will occur at $X_{Bf} \sim 300$ m and $X_{Mf} \sim 150$ m for neutral stability. From this it is apparent that the plume rise will be complete before x direction diffusion has much opportunity to smear out the transient mass release.

With these factors in mind it is suggested that a reasonably accurate estimate of plume rise can be made directly from the "frozen" mass emission rate without accounting explicitly for along-wind diffusion. The only exception to this is near the front of the plume where the high initial release rates rapidly diffuse downwind. To account for this it is suggested that the release rates for times less than some specified delay time t_d be taken as constant and equal to the release rate at this time. This is illustrated in the sketch below.

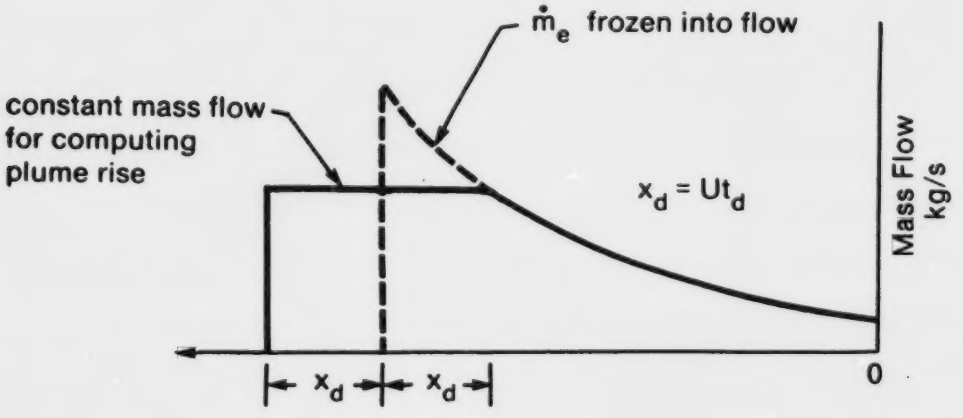

Considering that the initial release rate will be dissipated in blowing off the overburden from a buried pipeline, as well as dissipated by x direction diffusion, it is suggested that delay times t_d should lie in the range from 5 to 10 seconds.

Finally, because the final rise will occur very close to the point of rupture, the final rise equations 6-4 and 6-5 may be used at all x directions, rather than resorting to the additional complication involved in the transitional rise formulas 6-2 and 6-3.

Sensitivity of Ground Level Concentration to Plume Rise

Of all the factors effecting downwind concentration from a pipeline rupture, the plume rise is probably known with the least degree of certainty. The relevant question to ask then, is how sensitive the ground level concentration is to variations in plume rise.

For a ground level release, which has a zero source height, the effect of plume rise can be best understood by forming the ratio of ground level concentration with, and without plume rise. At a given downwind position this ratio is simply

$$\frac{c_o}{c_{o,\Delta h=o}} = \exp\left[\frac{-(\Delta h)^2}{2\sigma_z^2}\right] \qquad (6\text{-}10)$$

where c_o is the ground level concentration. This equation is plotted in Figure 6-1. It is apparent that in order to reduce ground level concentration to 60% or less of the value with no plume rise, the normalized source height must be at least $\Delta h > \sigma_z$. For plume rise greater than this value the ground level concentration is considerably reduced.

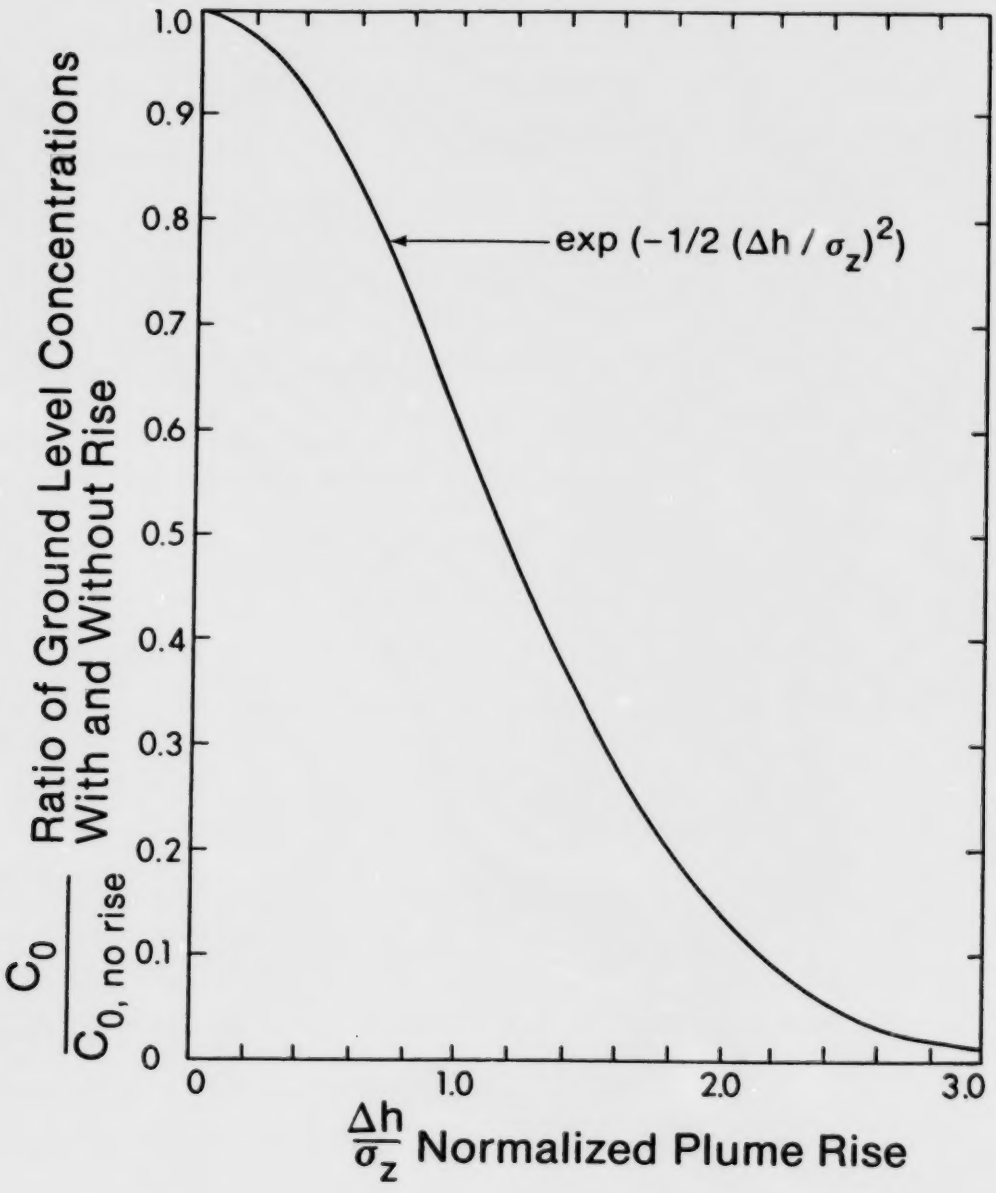

Figure 6-1 Effect of Plume Rise on Ground Level Concentration

For example, if the plume rise from the pipeline rupture is found to be $\Delta h \approx 20$ m and the vertical spreading rate in a neutrally stable atmosphere is $\sigma_z = 0.2\ x^{0.76}$, the condition that $\Delta h > \sigma_z$ is met only for $x < 420$ m. This indicates that plume rise will only have a significant effect on ground level concentration at locations close to the source, for a neutrally stable atmosphere.

In contrast, class F stability has $\sigma_z = 0.12\ x^{0.67}$ and $\Delta h > \sigma_z$ for $x < 2000$ m. This shows plume rise will have its maximum effect on ground level concentration for stable conditions. This is precisely the atmospheric condition that produces high ground level concentrations, indicating that plume rise may play a significant role in determining expected concentrations.

SECTION 7
SPREADING RATES OF PLUMES

In selecting spreading rates for plumes from a ground level pipeline rupture, the following factors must be taken into account:

1. The plume from a rupture is a short-term transient, which may not sample the entire range of atmospheric turbulent eddies. This will tend to reduce spreading rate of a plume closer to values that would be observed for single instantaneous puff.
2. The ground level release from pipeline rupture spreads in a region of high atmospheric turbulence in comparison to the plume from an elevated stack. This higher atmospheric turbulence level would tend to produce larger plume spreading rates than the accepted correlations used for stack gas dispersion.
3. Because of the transient nature of a pipeline rupture, it is necessary to include the effects of along-wind dispersion which tends to smear out x direction variations.
4. The highly turbulent gas jet emitted from the pipeline rupture will have its own internally generated turbulence which will induce entrainment, and generate "self-dilution." Close to the source plume spreading from internally generated turbulence may have a significant effect on ground level concentration. In fact, we will later show that this self-generated turbulence is not an important factor in determining ground level concentration, and may be neglected in all practical applications.

Vertical Plume Spread, σ_z

Because most correlation methods for predicting plume spreading rates do not include an explicit term to account for atmospheric turbulence,

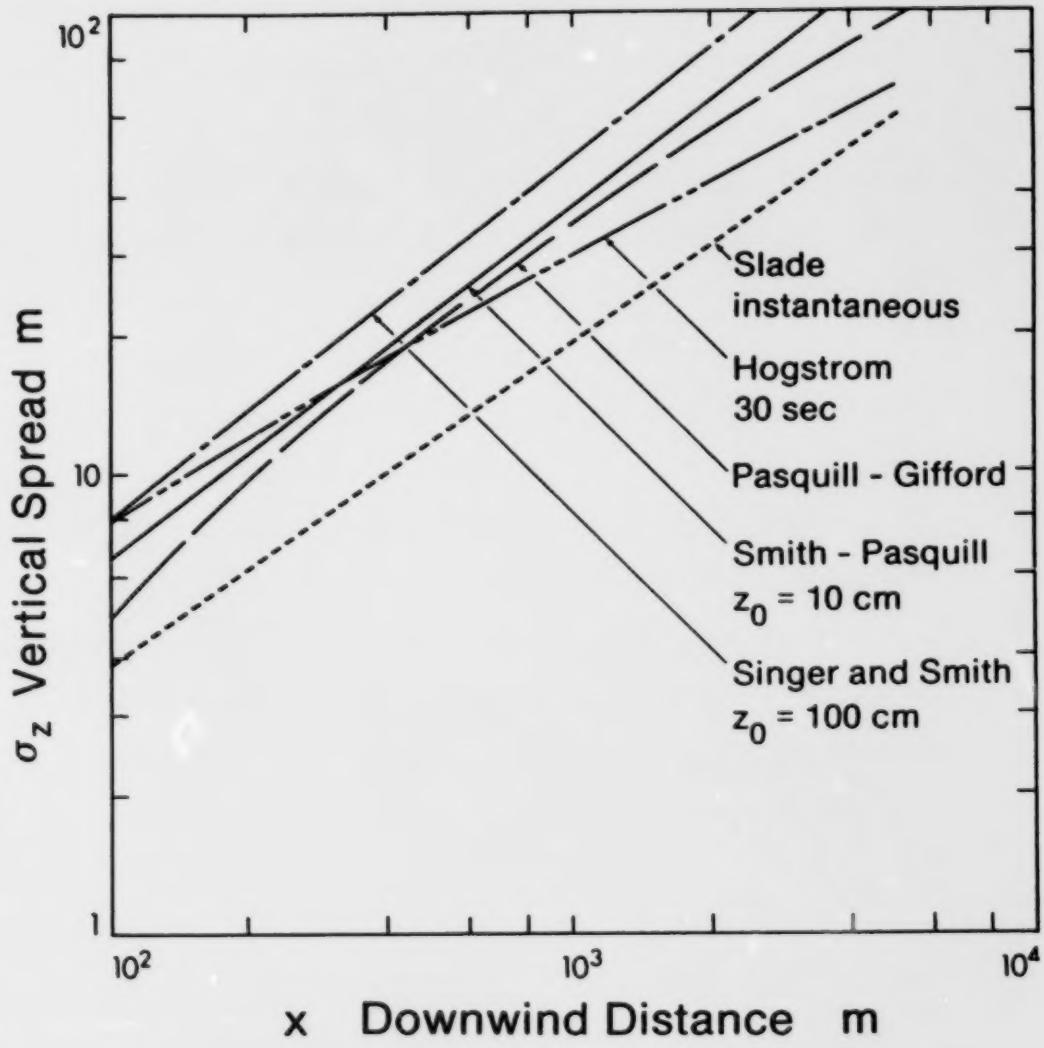

Figure 7-1 Vertical Spreading in Neutral Stability

there is a considerable variation between the recommended predictions. Several of these predictions are shown for neutral atmospheric stability in Figure 7-1.

Hogstrom's (1964) correlation is particularly interesting because it represents a 30 second release, which is typical of the time constants for mass release rate from pipeline ruptures. This correlation supports the statement made by Hogstrom that even for relatively short duration releases of about 30 seconds, the spreading rates will be more typical of continuous plumes than of instantaneous sources, see for example the instantaneous release spreading rate of Slade (1968).

Because the increased spreading rate induced by high atmospheric turbulence near ground level will be compensated for by the reduced spreading rate due to the short release time for a pipeline rupture, it is suggested that the spreading rates for continuous elevated plumes will also apply for pipeline ruptures. The power-law equations of Smith, given by Pasquill (1975) are recommended as good "average" values. The power-law equations recommended by Smith also include a correction for the effects of changing surface roughness Z_o. The constants for various atmospheric stability and surface roughness conditions are tabulated in Table 7-1.

Crosswind Plume Spread σ_y

The crosswind plume spreading correlations of several authors are presented in Figure 7-2. Here, as was the case for vertical spreading, the correlation of Hogstrom for a 30 second release falls close to the continuous plume spreading rates, and considerably higher than Slade's recommendation for an instantaneous puff.

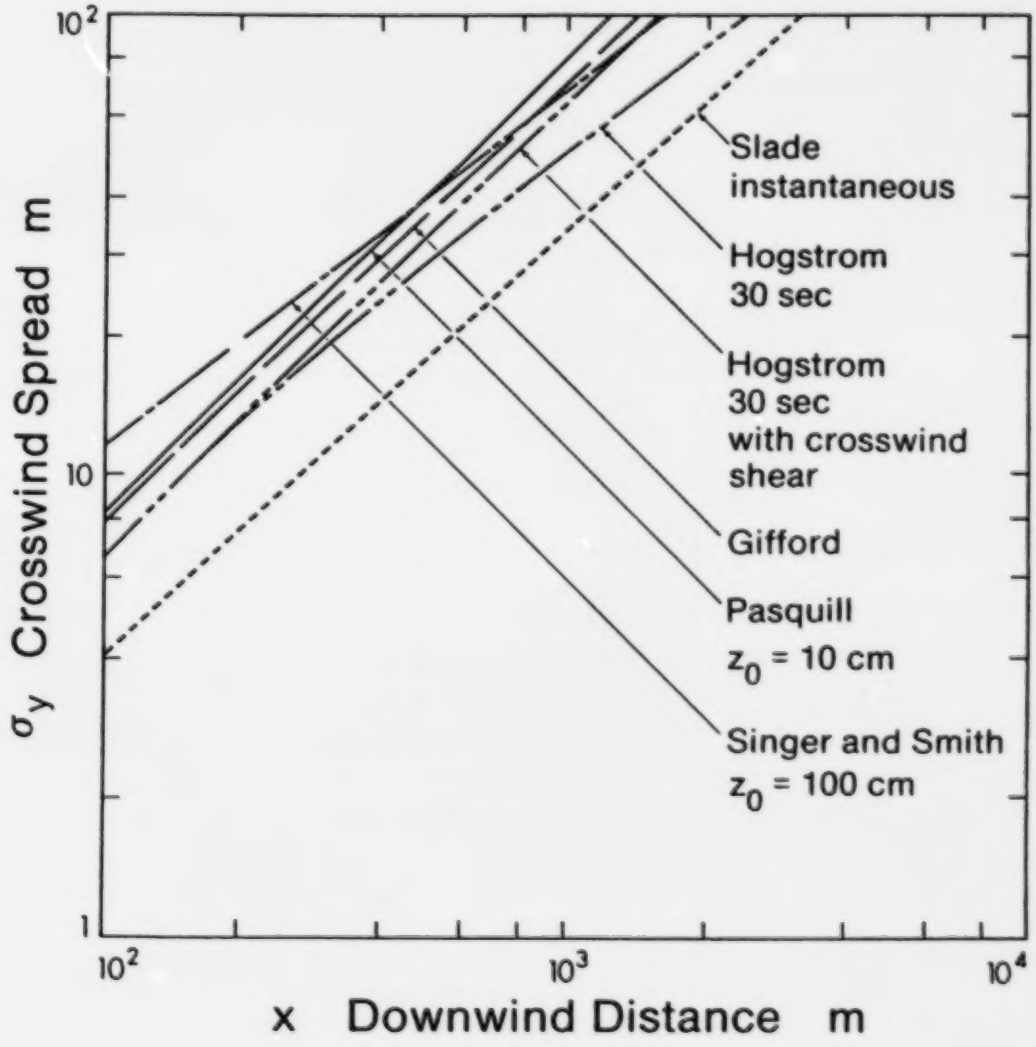

Figure 7-2 Crosswind Spreading in Neutral Stability

TABLE 7-1

PLUME SPREADING BY ATMOSPHERIC TURBULENCE

$$\sigma_y = A\, x^a \quad , \text{meters}$$

$$\sigma_z = B\, x^b \quad , \text{meters}$$

Atmospheric Stability	Pasquill Class	Surface Roughness Z_o c_m	Plume Spread Constants for x in meters				
			A	a	B	b	
Moderately unstable	B	10 cm 100 cm	0.38 0.48	0.87 0.87	0.23 0.54	0.85 0.77	
neutral	D	10 cm 100 cm	0.18 0.23	0.87 0.87	0.20 0.46	0.76 0.68	
Moderately stable	F	10 cm 100 cm	0.093 0.12	0.87 0.87	0.12 0.31	0.67 0.58	

1.) Crosswind spread σ_y for $Z_o \simeq 10$ cm from Gifford, Fig. 3-10 in Slade (ed.) (1968), Meteorology and Atomic Energy 1968 U.S. Atomic Energy Commission TID 24190. For $Z_o = 100$ cm A increased by 25% from $Z_o = 10$ cm

2.) Vertical spread, σ_z from Smith, Table 6.1 in Pasquill (1975) Atmospheric Diffusion Halsted Press

The crosswind spreading rates of Gifford (1968) are recommended as good "average" values. Unfortunately, none of the correlations account for the expected increase in spreading rate with increased terrain surface roughness Z_o. For a ground level release from a pipeline rupture, this increase in crosswind spreading rate due to mechanically generated surface turbulence must certainly exist to some extent. To account for this, it is suggested that Gifford's values be used for surface roughness of Z_o = 10 cm and that these values be increased by a factor of 1.25 for terrain with surface roughness of Z_o = 100 cm.

It is recommended that no correction be applied to crosswind spreading rates for the increased turbulence close to the ground or for the short release time for a pipeline rupture plume. The argument for making no correction for these effects is the same as for vertical spread; that the two effects will tend to cancel each other, and that not enough is known about either of these factors to allow quantitative corrections to be applied with any confidence.

The constants necessary for a power law representation of Gifford's crosswind plume spreading rates are given in Table 7-1, including the 25% correction for increased spread over rough terrain.

Along-Wind Plume Spread σ_x

Very little is known about spreading rates in the along-wind direction. For continuous plumes with steady release rates, it is impossible to measure this parameter.

As an additional complication, the variation of wind velocity with height will generate an along-wind dispersion which will be superposed on this spreading induced by background turbulence. Because the vertical

wind profile varies with atmospheric stability and with terrain roughness, it is suggested that a theoretical estimate be made for this effect.

For the simplest type of velocity profile, a linear variation of wind speed with height, several theoretical solutions for shear-induced dispersion are available. Smith (1965) gives a comprehensive review of the literature. All of the theoretical solutions have the general form

$$\sigma_x^2 = \left[\alpha_1 \left(\frac{dU}{dz} \cdot t\right)^2 + \alpha_2\right] \sigma_z^2 \qquad (7\text{-}1)$$

where

σ_z = vertical plume spread, m

σ_x = along-wind spread, m

$\frac{dU}{dz}$ = velocity gradient (constant for a linear velocity profile) sec^{-1}

t = time of plume travel, sec

α_1 = wind shear constant

α_2 = turbulence intensity and scale ratio for x and z components

Noting that the time of travel is just x/U and using the value of $\alpha_1 \cong 0.08$ developed by several investigators (see Smith (1965))

$$\sigma_x^2 = \left[0.08\left(\frac{dU}{dz} \cdot \frac{x}{U}\right)^2 + \alpha_2\right] \sigma_z^2 \qquad (7\text{-}2)$$

For a power law velocity profile where $U \propto z^n$ the velocity gradient is

$$\frac{dU}{dz} = \frac{nU}{z} \qquad (7\text{-}3)$$

For long downwind distance $\sigma_z \propto x^{1/2}$ and wind shear effects produce $\sigma_x \propto x^{3/2} \propto t^{3/2}$ which has been observed by several investigators, see Gifford (1977). To preserve this "classic" $t^{3/2}$ relation even when σ_z does not vary as $x^{1/2}$, the following form for 7-2 is suggested, using 7-3,

$$\sigma_x^2 = \left[0.08 \left(\frac{nx}{z_c} \right)^{3-2b} + \alpha_2 \right] \sigma_z^2 \qquad (7\text{-}4)$$

where σ_z is assumed to follow the power law in Table 7-1 in the form

$$\sigma_z = B\, x^b \qquad (7\text{-}5)$$

and z_c is some reference height for evaluating the velocity gradient.

The recommended values for the factor α_2 depend on the ratio between turbulence intensity and scale for vertical and along-wind components. The table below gives values which are approximate.

TABLE 7-2

Atmospheric Stability	Pasquill Class	α_2
Moderately Unstable	B	6
Neutral	D	8
Moderately Stable	F	10

The reference height z_c where the velocity gradient is evaluated, is somewhat arbitrary because the theory strictly applies only for a linear velocity profile. It is suggested that for a ground level release

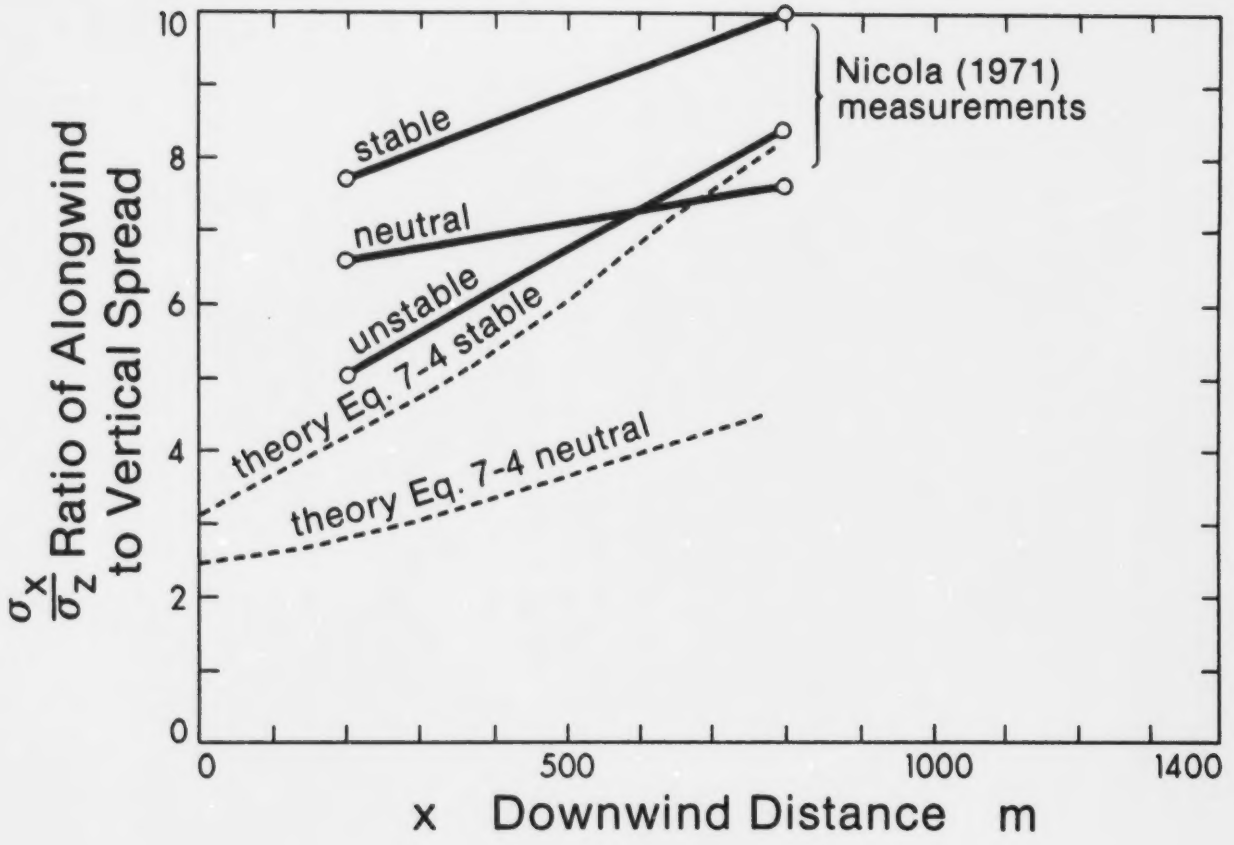

Figure 7-3 Ratio of Along-Wind to Vertical Spread

with no plume rise that this reference value be taken somewhere between 5 and 10 meters, and that with plume rise the reference height be evaluated midway between ground level and the plume center-line.

There is almost no data available with which to compare the recommended along-wind plume spread given by equation 7-4. The only experimental data that the author could find was that of Nickola (1971) who measured the ratio of along-wind to vertical dispersion for ground level releases. This data is shown in Figure 7-3, where it is compared with the predictions from equation 7-4. From this data, it would appear that the estimated along-wind spread will be somewhat underestimated by 7-4, giving conservatively high values for ground level concentration. Fortunately, ground level concentration is not particularly sensitive to the values chosen for the along-wind spread. The reason for this is that the x direction spreading simply redistributes material along the plume axis, rather than causing significant dilution as is the case for cross-wind and vertical spread. With this in mind, equation 7-4 is probably accurate enough for the purpose of estimating ground level concentrations from pipeline ruptures. In any case, it is certainly more accurate than the previous practice of setting along-wind spreading rates equal to crosswind rates.

Plume Spread from Self-Generated Turbulence

The additional plume spreading caused by entrainment from self-generated turbulence can be estimated in the following way:

The buoyancy and momentum induced plume rise depends on the rate of entrainment of ambient air into the plume. In all plume rise theories, this entrainment rate is assumed to be due to self-generated turbulence. A review of various plume rise theories is given by Briggs (1975). Most

of the theories which are successful in correlating observed plume rise use Taylor's entrainment hypothesis, which states simply that the radius of the plume increases linearly with its height above the source

$$R = \beta \cdot \Delta h + R_o \qquad (7\text{-}6)$$

R = plume radius, m

β = entrainment constant, typically β = 0.6 to 0.9

R_o = initial plume radius at the source

In addition, most plume rise theories assume a rectangular "top-hat" profile for the concentration inside the plume. The plume radius is simply the distance to the edge of this top-hat profile.

Because the actual plume profile is a Gaussian, some relationship between the Gaussian standard deviation σ_s the spread due to self-generated turbulence, and the plume radius R must be developed. One simple assumption is to use a Gaussian with the same center-Line concentration as the top hat profile. For this case we find that for the same mass flux through a top hat and Gaussian profile the plume radius is simply $R = \sqrt{2}\,\sigma_s$. Another alternative used by Slawson (1977) and others is to take the plume radius R at the point where the concentration in the Gaussian has been reduced to 10 percent of the center-line value. For this case it is found that the plume radius is $R = 2.15\,\sigma_s$.

For the present analysis we will assume that the plume radius is given by $R = 2\,\sigma_s$. Using this,Taylor's entrainment hypothesis from equation 7-6 simply becomes

$$\sigma_s = \frac{\beta}{2} \cdot \Delta h + \frac{R_o}{2} \qquad (7\text{-}7)$$

Because the self-generated turbulent spreading is uncorrelated with entrainment due to atmospheric turbulence, their variances may be added to give the total spreading rate as

$$\sigma_{zt}^2 = \sigma_z^2 + \sigma_s^2 \tag{7-8}$$

which, assuming that R_o is small can be written using 7-7 as

$$\sigma_{zt}^2 = \sigma_z^2 + \frac{\beta^2}{4} \cdot \Delta h^2 \tag{7-9}$$

where

σ_{zt} = total plume spread, m

σ_z = plume spread by atmospheric turbulence , m

In order to test the sensitivity of ground level concentrations to the effect of self-generated plume spread, a sample calculation was carried out for a ground level release. A typical value of $\beta^2 = 0.5$ was used for the entrainment constant. It was found that the ratio of ground level concentration with self-generated spreading, to that without spreading, depended only on the normalized plume rise $\Delta h/\sigma_z$. The calculation yielded the rather surprising result that self-generated spreading causes the ground level concentration to increase. This is logical, because the additional spreading reduces concentration at the plume center line by diffusing it toward ground level. It was found that a significant effect (>30%) on ground level concentration occurred when the non-dimensional plume height was greater than about 1.5. In the case of a pipeline rupture, assuming a plume rise of 20 meters as a typical value,

the preceding calculation indicated that self-generated turbulence spread would cease to have any significanct effect beyond a distance of 100 to 200 meters from the source, depending on atmospheric stability. It is suggested that this effect be neglected for all pipeline rupture calculations.

All of the preceeding analysis assumed implicitly that the jet of gas was directed vertically at the point of release. For a horizontal gas jet there will be no momentum rise, but momentum effects will still cause jet entraiment and self-dilution. Because jet entraiment is not linked to plume rise for a horizontal release, estimates of the effect of this entraiment on ground level concentration require a different type of analysis.

SECTION 8
INDOOR-OUTDOOR CONCENTRATION RATIOS

It has been estimated that in cool climates, we spend as much as 95% of our lives indoors. Even on a warm summer day our jobs, combined with force of habit, keep a large majority of any urban population indoors. Because it is precisely the risk of pipeline rupture near such concentrated urban areas that presents the greatest danger to loss of human life, we must examine how this tendency to remain inside buildings influences the concentration that a person will be exposed to.

The idea that buildings protect people from air pollution is not a new one. For example Halpern (1978) and Thompson et al (1973) present indoor-outdoor exposure levels for various air pollutants. Figure 8-1 shows a typical indoor-outdoor concentration ratio for particulate concentration levels measured in an urban area by Yocom et al (1971). The concentration ratio shown in this figure indicates as expected that in winter, when buildings are isolated from the outside by keeping windows and doors closed, indoor concentrations are much less than outdoor levels. As expected, the largest indoor concentrations are observed in summer, when windows and doors are left open for natural ventilation.

Because of the random variation in outside concentrations of pollutants such as particulate matter, it is very difficult to establish any quantitative predictions for indoor-outdoor ratios. Also, the measurements reported in the literature are all concerned with relatively long-time transients, which have a period of hours or days, so there is only a tenuous analogy between any of these measured concentration ratios and the present problem which is concerned with a short duration transient.

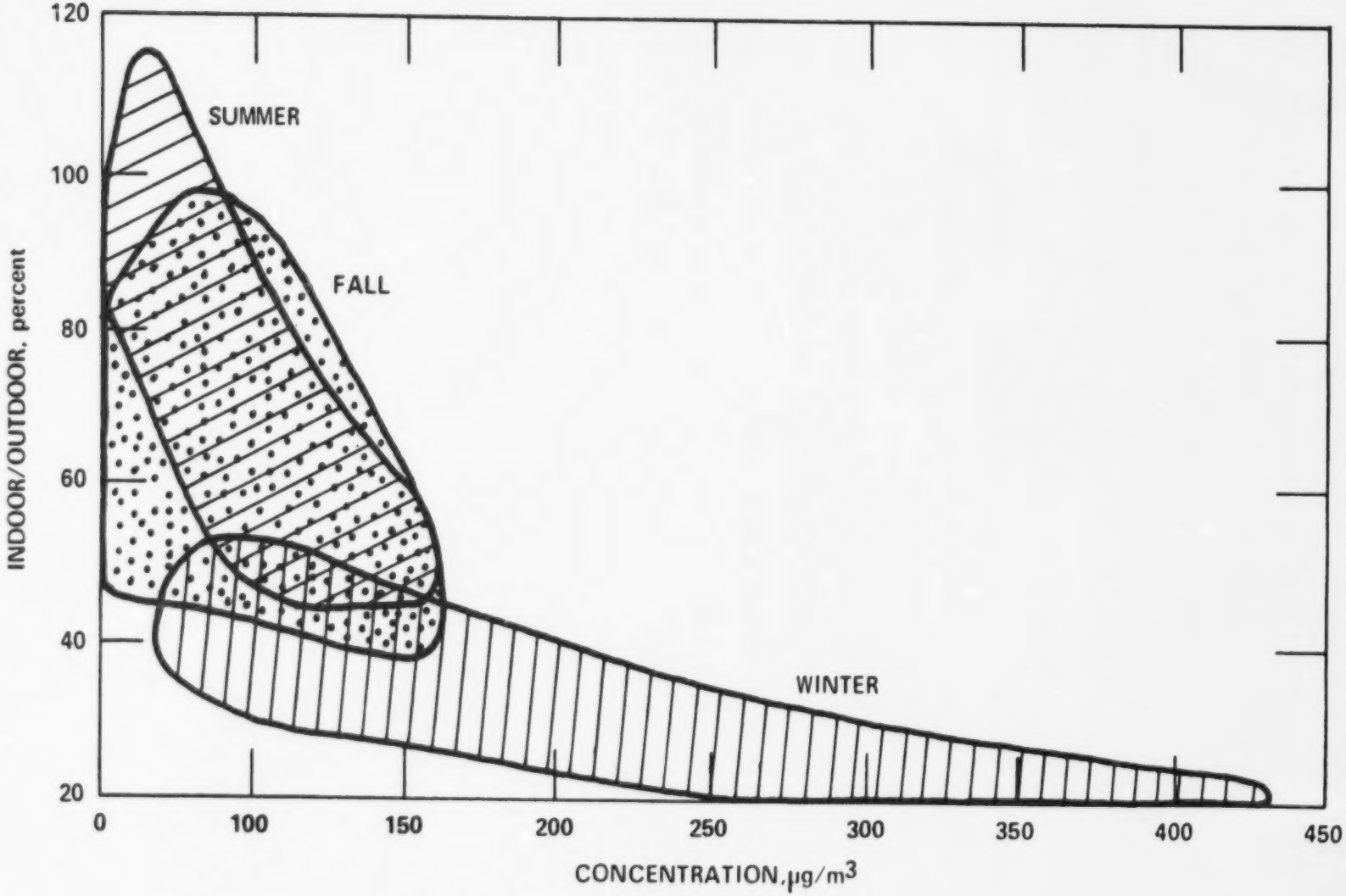

Figure 8-1 Seasonal Variation of Particulate Concentration and Indoor/Outdoor Ratios in Hartford, Connecticut from Benson, Anderson and Caldwell (1972).

Analytical Modelling for Indoor-Outdoor Ratios

In the case of a pipeline rupture, the functional form of the time varying outdoor concentration as it passes over a building is usually known, and can be represented by an exponential decay, or a series of exponentials. This known functional form is in contrast to the random variations of the outdoor levels of most air pollutants. With this known functional form, it is possible to compute the indoor concentration level if the rate of infiltration of outdoor air is known.

In the following analysis we will model the building by the classical approximation of "well-stirred tank." With this approximation any outside concentration which infiltrates the building through windows, or by direct aspiration through ventilation systems, is mixed immediately and completely with all the air in the building to produce a uniform inside averaged concentration level. This approximation is shown in Figure 8-2 where in order to maintain a constant amount of air inside the building, the rate of outflow which carries with it the average concentration must be equal to the infiltration rate which brings with it a time varying outdoor concentration level. This infiltration rate $\dot{v}$ is assumed to be constant over the time interval during which the transient plume from the pipeline rupture passes over the building.

The mass balance of the material represented by concentration c (in our case hydrogen sulphide) is given by

$$\begin{matrix}\text{increase of mass} \\ \text{inside building}\end{matrix} = \begin{matrix}\text{mass} \\ \text{inflow}\end{matrix} - \begin{matrix}\text{mass} \\ \text{outflow}\end{matrix}$$

$$V d\bar{c} = c(t')\, \dot{v}\, dt' - \bar{c}\, \dot{v}\, dt'$$

which gives the differential equation

$$\tau_B \frac{d\bar{c}}{dt'} + \bar{c} = c(t') \qquad (8\text{-}1)$$

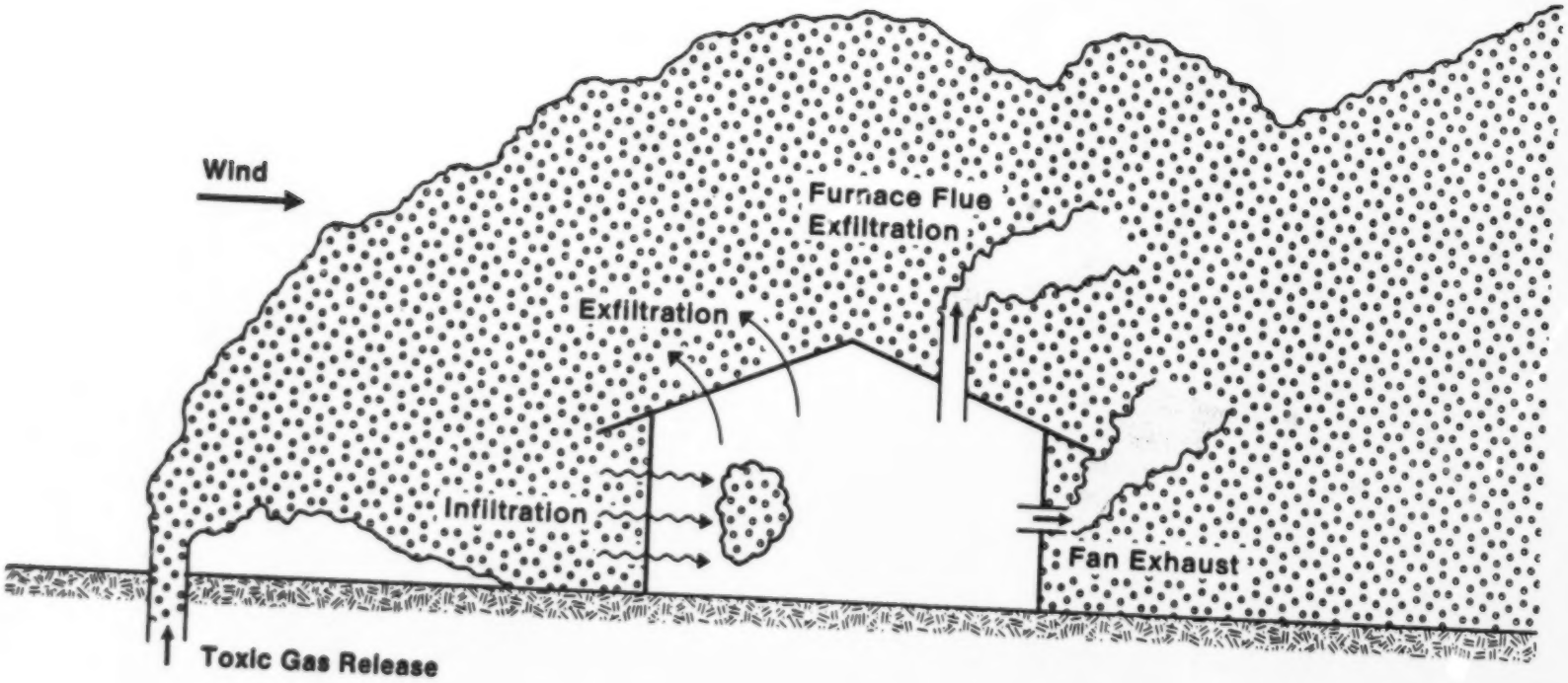

Figure 8-2 Infiltration of Contaminated Outside Air Into a Building

where, (see Figure 8-2)

$\bar{c}$ = the inside 'well-stirred" average concentration kg/m^3

$c(t')$ = time varying outdoor concentration kg/m^3

V = internal mixed volume of building, excluding stagnant air spaces, m^3

$\dot{v}$ = infiltration (and outflow) rate m^3/s

τ_B = building time constant, sec.

t' = time after plume from rupture arrives at the building, sec.

The building time constant is simply the time required for one complete air change of the mixed volume V to take place and is given by

$$\tau_B = \frac{V}{\dot{v}} \tag{8-2}$$

This time constant is often expressed as the number of air changes per hour.

The general solution of equation 8-1 for any time varying concentration that has $c(t') = 0$ for all times $t' < 0$ is given by

$$\bar{c}\,(t') = \exp\left(\frac{-t'}{\tau_B}\right) \int_0^{t'} \frac{c(t')}{\tau_B} \exp\left(\frac{t'}{\tau_B}\right)\, dt' \tag{8-3}$$

A specific solution of equation (8-3) appropriate for pipeline ruptures will be given below.

Exponential Decay of Outdooor Concentration

Because the release rate from a pipeline rupture can be described by an exponential, or a series of exponentials, the indoor concentration for this type of outdoor variation can now be computed. Because a series of exponentials can be integrated term by term in equation 8-3, it is only necessary to consider here a single exponential of the form

$$c = c_o \exp\left(\frac{-t'}{\tau}\right) \tag{8-4}$$

where

c = outdoor concentration at time t'

c_o = outdoor concentration when the plume arrives at t' = 0

τ = decay time constant of outdoor concentration

When equation 8-4 is inserted in 8-3 and the integral evaluated, the indoor-outdoor concentration relationship is given by

$$\frac{\bar{c}}{c_o} = \frac{1}{\left(\frac{\tau_B}{\tau} - 1\right)}\left[\exp\left(\frac{-t'}{\tau_B}\right) - \exp\left(\frac{-t'}{\tau}\right)\right] \tag{8-5}$$

In equation 8-5 the time constant for the transient variation of the outdoor concentration must be determined by the release rate, and the analysis of along-wind dispersion effect. The building time constant in terms of its air changes per hour is much more difficult to determine, and will vary considerably from building to building and with time of year.

Building Infiltration Rates

In order to evaluate the rates of change of building air, a great deal of value judgement must be applied in selecting some "recommended" values. For example, in summer, office buildings which rely on internal air conditioning have much lower infiltration rates than apartments or single family housing which depends on natural ventilation through open windows. In winter infiltration levels in all buildings is at a minimum, with doors and windows closed, with the main source of infiltration consisting of make-up air to replace that used in combustion for space heating.

With all these factors in mind, about all that can be done is to estimate the order of magnitude of infiltration rates. One set of estimated values used as a guideline for air conditioning design is given below.

TABLE 8-1

Air Changes Occurring Under Average Conditions in Residences, Exclusive of Air Provided for Ventilation[a]

Kind of room	Number of Air Changes per hour
Rooms with no windows or exterior doors	0.5
Rooms with windows or exterior doors on one side	1
Rooms with windows or exterior doors on two sides	1.5
Rooms with windows or exterior doors on three sides	2
Entrance halls	2

[a] For rooms with weatherstripped windows or with storm sash, use two-thirds these values.

from American Society of Heating Refrigeration and Air-Conditioning Enginers Handbook of Fundamentals Chapter 21 Section 5 (1977).

One major uncertainty associated with infiltration of toxic gases from pipeline ruptures into buildings is the assumption of a "well-stirred tank." In fact, in entryways and near open windows the air entering from outside will certainly not be immediately mixed to an average indoor concentration. Furthermore, in the short time interval during which the plume from the pipeline rupture passes over the building, many rooms may remain sealed and the internal effective mixing volume of the building may be much smaller than its total volume for a long duration outside concentration

To account for these factors it is suggested that much higher infiltration rates be assumed than are normally used for ventilation design purposes. Because the use of air conditioning systems is not widespread in Alberta, it will be assumed that in spring and summer many windows will be opened to afford natural ventilation. The recommended values for

infiltration time constants are given in Table 8-2 below.

TABLE 8-2

RECOMMENDED INFILTRATION TIME CONSTANTS

Season	τ_t	
	seconds	air changes/hr
spring and summer	360	10
fall and winter	900	4

The values in Table 8-2 contain a considerable component of subjective judgement in their selection. If anything, they are probably somewhat conservative (that is too high)and will predict larger indoor concentrations than will actually occur. In making use of these time constants, it should be kept firmly in mind that a person standing a few meters away from a wide open window in a room with good cross-ventilation is, to all intents and purposes, outdoors. It is only in relatively large buildings, and away from open doors and windows that the building internal mixing volume will act to damp out the sudden changes in outside concentration during transient releases from pipeline ruptures.

Maximum Indoor Concentration

For an exponentially decaying outdoor concentration, the indoor concentration will rise, reach a peak value, and then die away. The time at which this maximum indoor concentration occurs can be determined by taking the derivitive of equation 8-5 equating it to zero, and solving for the maximum point. Carrying out this procedure, the time at which the indoor concentration reaches a maximum is given by

$$t'_{max} = \frac{\ln\left(\frac{\tau_B}{\tau}\right)}{\left(\frac{1}{\tau} - \frac{1}{\tau_B}\right)} \qquad (8\text{-}6)$$

By inserting equation 8-6 into 8-5 the maximum indoor concentration can be computed directly, without having to follow the time history of the indoor concentration variations.

Effect of Outdoor Concentration Fluctuations

In addition to the exponential time decay of outdoor concentration, there will be rapid random fluctuations due to the turbulent diffusion processes. In order to assess the effect of an outdoor fluctuation on the indoor average concentration, an analysis was carried out for a sinusoidally varying outside concentration with a fixed frequency. This would correspond to a single Fourier component of the concentration fluctuation spectrum.

The analysis is only approximate in nature because the process is not stationary, that is it does not have a steady average, but rather is decaying exponentially with time. The simple analysis showed that for a concentration fluctuation frequency of 0.1 H_z and a building time constant of τ_B = 360 sec, the amplitude inside the building would be about 0.1% of the outside value. In other words, for all practical purposes the effect of a building is to completely remove any rapid time fluctuations in outside concentration.

Numerical Example

A numerical example was carried out using equation 8-5 for an exponentially decaying outdoor concentration. A rapid infiltration rate of 10 air changes per hour was assumed, and an outdoor time constant of

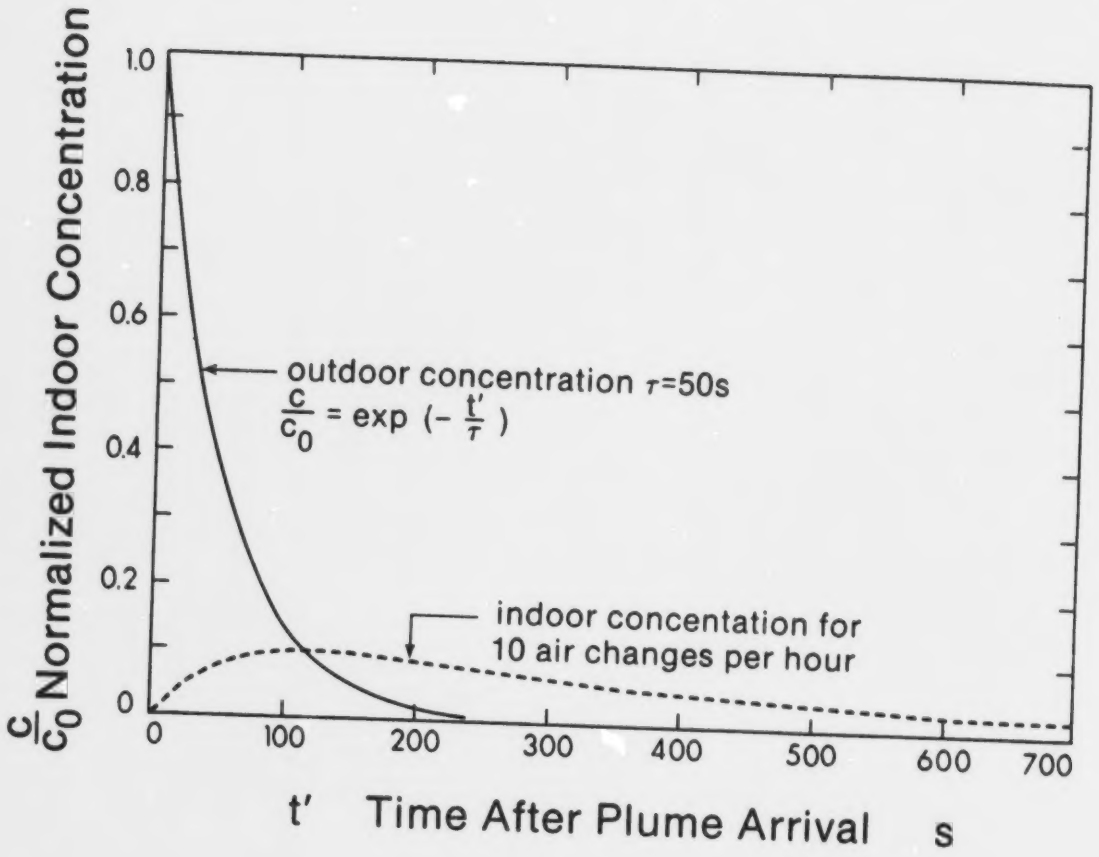

Figure 8-3 Indoor-Outdoor Concentrations for Exponential Outdoor Time Variation

50 seconds was used. Figure 8-3 shows the indoor-outdoor concentrations. For this sample case, the indoor concentration reached a level only 10% of the maximum outdoor concentration. Because of the internal volume in the building, the inside concentration level exceeded the outdoor concentration after about 100 seconds, and significant indoor levels were still being observed 700 seconds later, long after the transient plume had passed over the building, and the outside concentration returned again to zero.

From the preceding analysis, it can be concluded that because people spend most of their time indoors, there is significantly lower risk of exposure to high concentrations than atmospheric dispersion calculations would indicate. In particular, groups that would be termed "high-risk", including infants, the elderly, and people with chronic illness, would be even more likely to be found indoors and receive much lower exposure. Thus, in what would appear to be a self-contradictory statement, those in high risk health categories, are probably in a low risk of exposure category simply because they are indoors.

SECTION 9
CONCENTRATION FLUCTUATIONS AND PROBABILITY DISTRIBUTIONS

In any risk analysis it is essential to know the probability of occurrence of concentrations which are higher and lower than the mean value, which is predicted by the procedures outlined in the preceding sections. This is particularly true when even a single breath of a toxic gas is sufficient to cause a fatality. An example is shown graphically in Figure 9-1, where it can be seen that for the particular situation shown, the risk of fatality is very high, even though the mean concentration is much lower than the peak value.

Because the average concentration will vary with time due to the unsteady nature of the pipeline rupture mass release, the "mean" concentration represents an ensemble average taken over many successive pipe rupture releases into the same atmospheric conditions. Obviously, this ensemble average will never be observed in practice, when only a single release occurs.

The determination of the probability of observing a given concentration if the ensemble mean value is known has been investigated by Csanady who summarizes several of his studies in his 1973 book. The analysis presented in this section draws heavily from Csanady's work.

Log-normal Probability Distribution

If we consider the dilution of a puff of gas as a series of discrete steps rather than a continuous process, it is logical to assume that at each succeeding step in the dilution process the amount of ambient air which is entrained by a puff is directly proportional to the present volume of the puff. Thus, the dilution process is made up of a series

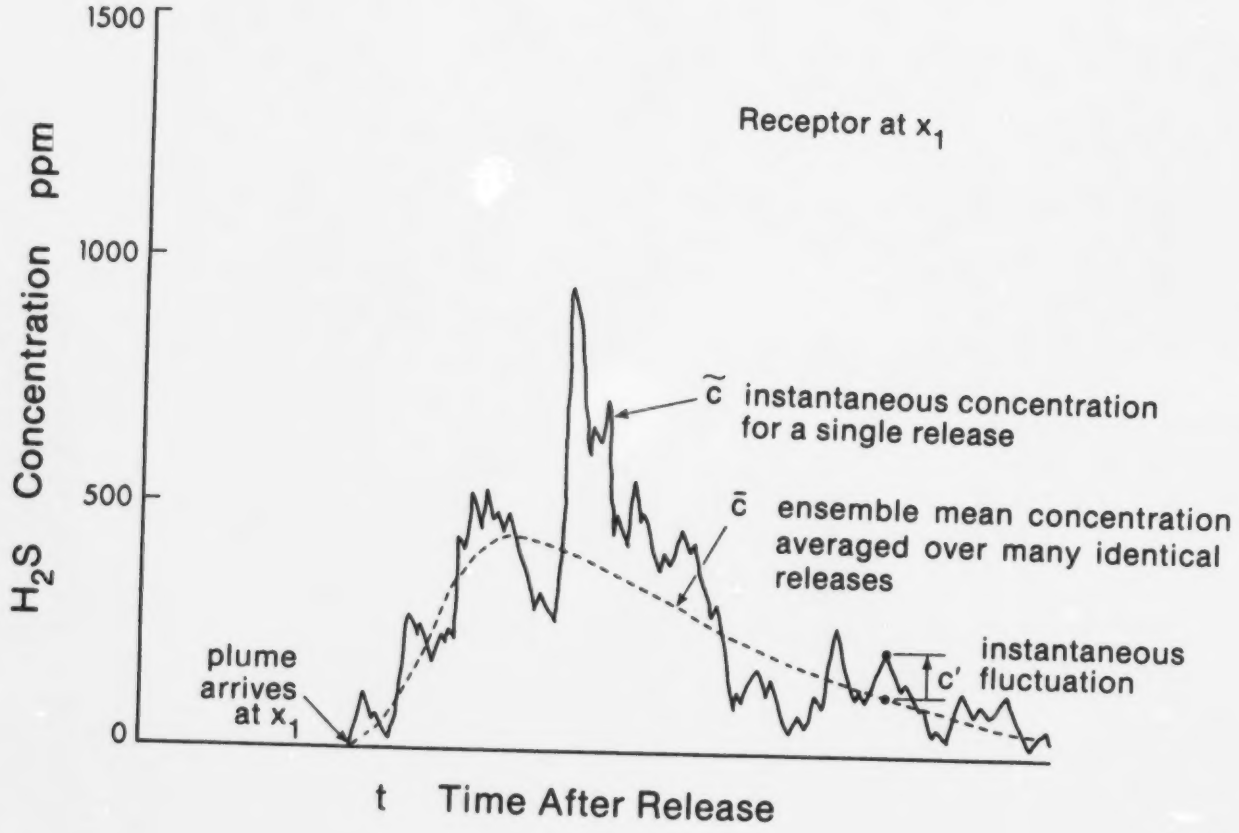

Figure 9-1 Ensemble Mean and Instantaneous Concentrations for a Time-Varying Source Release Rate

of random steps in which the preceding puff volume is multiplied by a random factor. Because the dilution process is a series of successive products rather than sums of random factors, it will be the logarithm of the concentration that will have a normal (Gaussian) probability distribution. Csanady (1973) p 228 gives the cumulative log-normal probability distribution as

$$\Omega\left(\frac{\tilde{c}}{c}\right) = \frac{1}{2}\left[1 + \text{erf}\left[\frac{\ln\left[\left(\frac{\tilde{c}}{c}\right)\exp\left(\frac{\sigma_1^2}{2}\right)\right]}{\sqrt{2}\,\sigma_1}\right]\right] \tag{9-1}$$

where

$\tilde{c}$ = concentration at any instant kg/m^3

c = mean concentration ensemble averaged kg/m^3

$\Omega(\frac{\tilde{c}}{c})$ = probability of observing a concentration less than $\tilde{c}/c$ at any instant

σ_1 = log standard deviation of distribution

The log standard deviation is given by

$$\sigma_1^2 = \ln\left[1 + i_c^2\right] \tag{9-2}$$

$$i_c^2 = \frac{\overline{c'^2}}{c^2} \tag{9-3}$$

where

$c' = (\tilde{c} - c)$, instantaneous deviation from the mean, see Fig. 9-1

$\overline{c'^2}$ = ensemble averaged variance

i_c = concentration fluctuation intensity

The probability density function $p\left(\frac{\tilde{c}}{c}\right) .d\left(\frac{\tilde{c}}{c}\right)$ is the probability of observing a concentration in the range from $\tilde{c}$ to $\tilde{c} + d\tilde{c}$ and is simply the derivative of the cumulative distribution

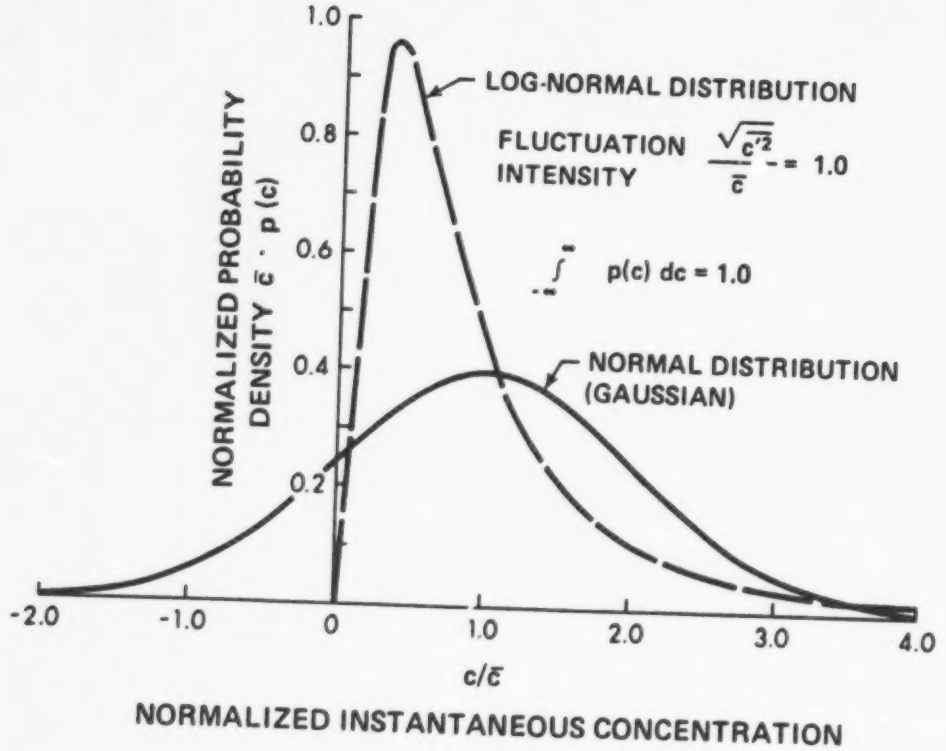

Figure 9-2 Comparison of Normal and Log-Normal Probability Densities for $i_c = 1.0$

$$p\left(\frac{\tilde{c}}{c}\right) = \frac{d\,\Omega}{d\left(\frac{\tilde{c}}{c}\right)} \qquad (9\text{-}4)$$

This probability density function p is shown in Figure 9-2 for both a log-normal, and a normal distribution with the same standard deviation. The log-normal distribution is highly skewed, predicting much higher probabilities of low concentrations than a Gaussian with the same variance. It is clear from Figure 9-2 that the normal distribution is not realistic, because it predicts negative concentrations.

Fluctuation Intensity Along the Plume Center Line

There is very little information on fluctuation intensity levels i_c in the atmosphere. Csanady (1973) suggests that the fluctuation intensity will vary with background turbulence, and therefore with the terrain roughness Z_o, as well as the atmospheric stability.

Recent unpublished wind tunnel experiments by Netterville (1978) show that fluctuation intensities are somewhat higher than those suggested by Csnady (1973), and that in addition the fluctuation intensity decays gradually as the plume moves downwind. Using these experiments as well as Csnady's recommendations the table below gives suggested values for the center-line fluctuation intensity.

TABLE 9-1

GROUND LEVEL*FLUCTUATION INTENSITY ON PLUME CENTERLINE

Atmospheric Stability	Pasquill Class	Centerline Intensity i_{co}	
		Z_o = 10 cm	Z_o = 100 cm
moderately unstable	B	0.5	1.0
neutral	D	0.5	1.0
moderately stable	F	0.25	0.5

*The ground surface tends to damp out fluctuations. For a receptor far above the ground surface, the values above should be doubled.

No attempt has been made to account for the gradual decay of fluctuation intensity with downwind distance. Until more data are available the decrease in fluctuation intensity with downwind distance should be regarded as a safety factor. The fluctuation intensities given in Table 9-1 should be appropriate in the range from about 500 m to 2000 m.

At locations closer to the source than 500 m, the log-normal probability distribution is only an approximate representation of the dilution process, and the intensities in Table 9-1 should be increased by about a factor of 2 to account for uncertainties near the source.

Crosswind Variations in Fluctuation Intensity

If we move off the plume centerline in a crosswind direction, the mean concentration rapidly decreases. The fluctuation intensity i_c will increase as the edge of the plume is approached, and high fluctuations ranging from centerline concentration to zero will occur.

Recent wind tunnel experiments by Netterville (1978) have shown that the concentration fluctuations are transported in much the same way as the mean concentration itself. In fact, the distribution of concentration fluctuations across the plume follows a Gaussian distribution with the same plume standard deviation as the mean concentration field. The variation of the concentration variance is simply

$$\overline{c'^2} = \overline{c_o'^2} \exp\left(\frac{-y^2}{2\sigma_y^2}\right) \qquad (9\text{-}5)$$

Because the mean concentration c is also a Gaussian

$$c = c_o \exp\left(\frac{-y^2}{2\sigma_y^2}\right) \qquad (9\text{-}6)$$

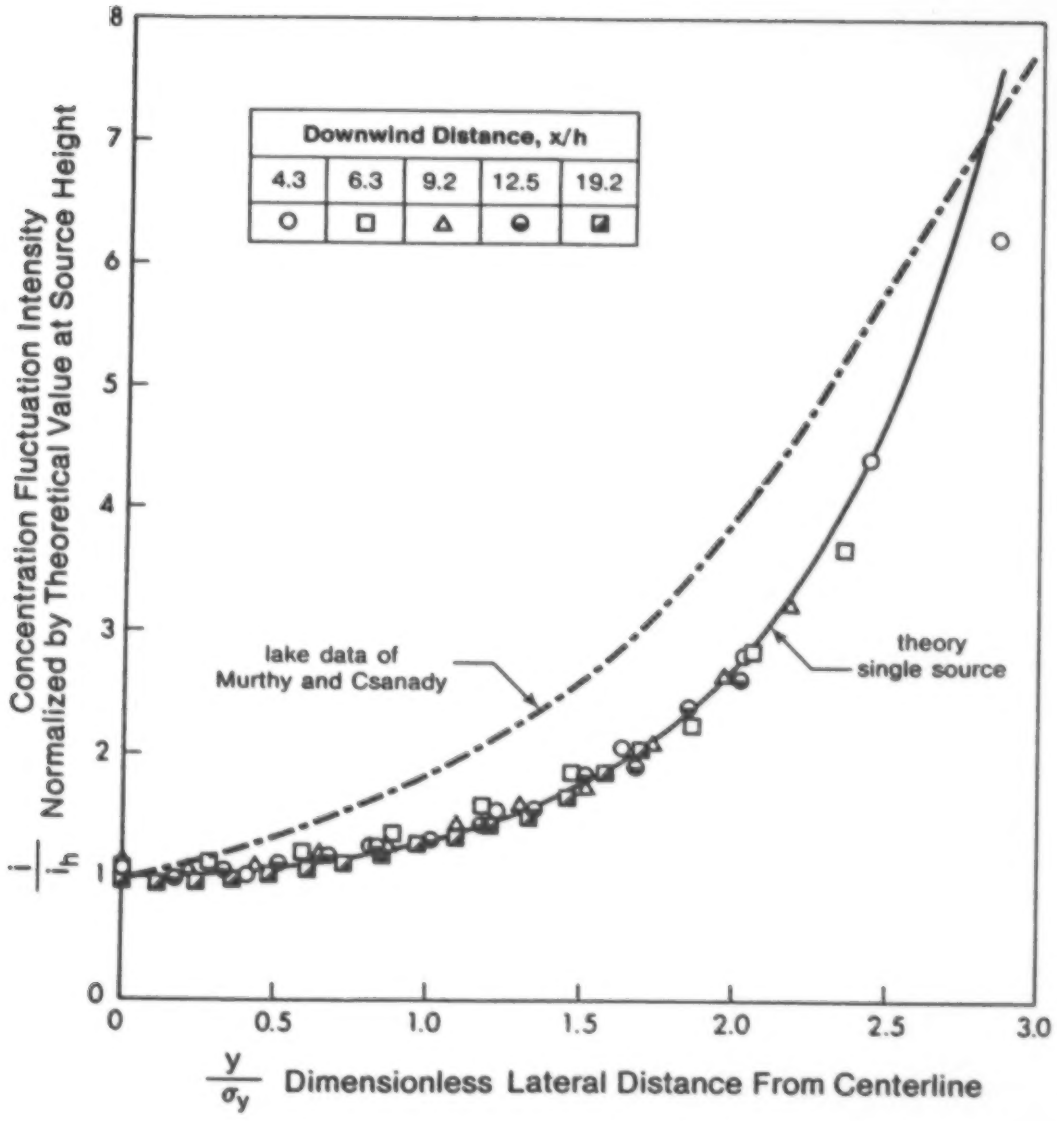

Figure 9-3 Measured and Predicted Crosswind Variations of Fluctuation Intensity

Then fluctuation intensity is simply

$$i_c = \frac{\sqrt{\overline{c'^2}}}{c} = i_{co} \exp\left(\frac{y^2}{4\sigma_y^2}\right) \qquad (9\text{-}7)$$

where

$\overline{c_o'^2}$ = concentration variance on plume centerline, kg^2/m^6

c_o = mean (ensemble averaged) concentration on plume centerline, kg/m^3

$i_{co} = \sqrt{\overline{c_o'^2}} \,/\, c_o$, fluctuation intensity on plume centerline

y = crosswind distance from plume centerline, m

σ_y = crosswind plume spread (standard deviation), m

The crosswind variation of fluctuation intensity is shown in Figure 9-3. It shows excellent agreement with the simple Gaussian equation 9-7.

Numerical Example

The probability of observing a concentration less than some specified value can be computed using equations 9-1, 9-2, and 9-7, and the recommended values for centerline fluctuation intensity in Table 9-1. It must be emphasized that the probability computed in this way represents the probability of occurrence of a single event at one instant of time. In more familiar terms, equation 9-1 represents the probability of having concentrations less than a specified value $\bar{c}$ in a single breath of air.

In an actual situation involving pipeline rupture, a person will be subjected to a time varying concentration field over some time interval in which many breaths will be taken. The probability that any of these many breaths will contain a given concentration is much more complicated than the single event probability given in equation 9-1. This probability,

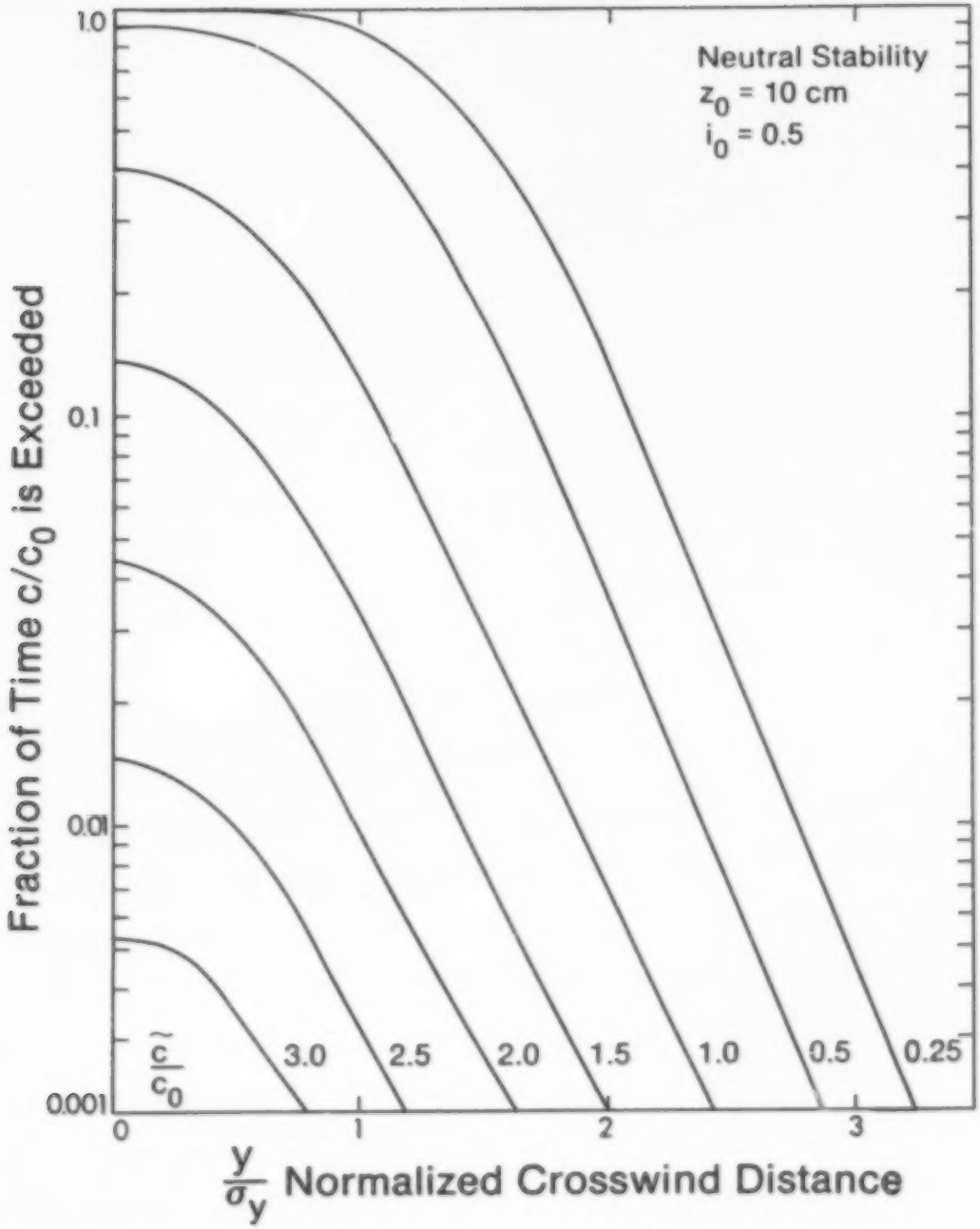

Figure 9-4 Probability of a Log-Normal Instantaneous Concentration $\tilde{C}$ Exceeding the Centerline Mean Concentration C_0 for Varying Distances Off Plume Centerline. Equation 8-8 with Neutral Stability, Surface Release into Z_0 = 10 cm Roughness, Centerline Fluctuation Intensity i_{co} = 0.5.

for a single event in many successive events exceeding a given concentration, must be considered in any risk analysis. It is beyond the scope of this investigation to develop this cumulative probability.

By combining equations 9-1, 9-6, and 9-7 the cumulative probability may be computed for a concentration normalized by the centerline mean concentration in the plume. This normalized probability is

$$\Omega\left(\frac{\bar{c}}{c_o}\right) = \frac{1}{2}\left[1 + \text{erf}\left[\frac{\ln\left(\frac{\bar{c}}{c_o}\right) + \frac{y^2}{2\sigma_y^2} + \frac{\sigma_1^2}{2}}{\sqrt{2}\,\sigma_1}\right]\right] \qquad (9\text{-}8)$$

Equation 9-8 represents the probability of the concentration being <u>less</u> than $\bar{c} / c_o$. The probability of <u>exceeding</u> $\bar{c} / c_o$ is simply $(1 - \Omega)$.

The probability of exceeding various specified multiples of the mean centerline concentration are given in Figure 9-4, for conditions of a neutrally stable atmosphere and a Z_o of 10 centimeters. A specific example for the use of this chart is given below.

The concentration at ground level on the plume centerline is c_o = 200 ppm of H_2S. At this x location the crosswind plume spread is σ_y = 50 m. What is the probability of the instantaneous concentration exceeding 400 ppm at a distance of y = 25 m off the centerline?

This probability may be computed as $(1 - \Omega)$ directly from equation 9-8. Alternately, by using Figure 9-4, the crosswind distance off the centerline and the peak to centerline concentration ratios are

$$\frac{y}{\sigma_y} = \frac{25}{50} = 0.5 \quad \text{and} \quad \frac{\bar{c}}{c_o} = \frac{400}{200} = 2$$

From Figure 9-4 the probability <u>at any one instant</u> for 400 ppm to be observed is found as $(1 - \Omega) = 0.029$.

The probabilities generated in this way can be used in a risk analysis to determine the probability that any given concentration (for example one that would cause a fatal dose) occurs at any point downwind.

References

Abramowitz, M. and Stegun, I. (eds.) (1965), Handbook of Mathematical Functions, Dover pp 297-311.

Bell, R.P. (1978), "Isopleth Calculations for Ruptures in Sour Gas Pipelines", Energy Processing/Canada, July-August 1978, pp 36-39.

Benson, F.B., Henderson, J.J. and Caldwell, D.E. (1972), "Indoor-Outdoor Air Pollution Relationships: A Literature Review", U.S. E.P.A. Publication AP-112.

Briggs, G.A. (1975) "Plume Rise Predictions" in Lectures on Air Pollution and Environmental Impact Analyses, Workshop sponsored by Am. Met. Soc., Boston, Mass., October 1975, pp 59-111.

Chuang, H. and Cermak, J.E. (1969), "Power Law Profiles in Thermally Stratified Shear Flows", Journal of Aircraft 6, PP 71-72.

Csanady, G.T. (1969), "Dosage Probabilities and Area Coverage from Instantaneous Point Sources at Ground Level", Atmos. Environment 3, pp 25-46.

Csanady, G.T. (1973), Turbulent Diffusion in the Environment, Reidel

Gifford, F.A. (1977), "Tropospheric Relative Diffusion Observations", Journal of Applied Met. 16, pp 311-313.

Geronimus, Yu. and Tseytlin, M. (1965), Tables of Integrals, Series and Products, 4th ed., Academic Press, pp 306-307.

Golder, D. (1972), "Relations Among Stability Parameters in the Surface Layer", Boundary Layer Meteorology 3, pp 47-58.

Halpern, M. (1978), "Indoor-Outdoor Pollution Exposure Continuity Relationships", Jour. Air Pollution Control Assn. 28, pp 689-691.

Hogstrom, V. (1964), "An Experimental Study on Atmospheric Diffusion", Tellus 16, pp 205-251.

Lott, R.A. (1977), "A Quasi-Steady Technique for Modeling the Atmospheric Dispersion of Continuous Plumes," T.V.A. Environmental Planning Division Preliminary Report.

Luna, R.E. and Church, H.W. (1971), "A Comparison of Turbulence Intensity and Stability Ratio Measurements to Pasquill Turbulence Types", Proc. American Met. Soc. Conference, Raleigh, N.C., April 1971, pp 35-39.

Netterville, D.D.J., (1978), PhD. Thesis (in progress)

Nickola, P.W. (1971), "Measurements of the Movement Concentration and Dimensions of Clouds Resulting from Instantaneous Point Sources", Jour. Applied Met. 10, pp 962-973.

Ricon, F.P. and Spalding, D.B. (1961), "Measurements of Entrainment by Axisymmetrical Turbulent Jets", Jour. Fluid Mechanics 11, pp 21-32.

Shapiro, A.M. (1953), The Dynamics and Thermodynamics of Compressible Fluid Flow, Volume 1, Ronald Press.

Slade, D.H. (ed.), Meteorology and Atomic Energy 1968, U.S. Atomic Energy - Div. of Tech. Information, TID-24190.

Slawson, P.R. (1978), "Observations and Predictions of Natural Draft Cooling Tower Plumes at Paradise Steam Plant", Atmos. Environment 12, pp 1713-1724.

Smith, F.B. and Hay, J.S. (1961), "The Expansion of Clusters of Particles in the Atmosphere", Quart. Jour. Royal Met. Soc. 87, pp 82-101.

Smith, F.B. (1965) "The Role of Wind Shear in Horizontal Diffusion of Ambient Particles", Quart. Jour. Roy. Met. Soc. 91, pp 318-329.

Thompson, C.R., Hensel, E.G. and Kats, G. (1973), "Outdoor-Indoor Levels of Six Air Pollutants", Jour. Air Pollution Control Assn. 23, pp 881-886.

Touma, J.S. (1977), "Dependence of the Wind Profile Power Law on Stability for Various Locations", Jour. Air Poll. Control Assn. 27, pp 863-866.

Yocom, J.E. Clink, W.L. and Cote, W.A. (1971), "Indoor-Outdoor Air Quality Relationships, Jour. Air Pollution Control Assn. 21, pp 251-259.